

1 Geographically divergent trends in ~~snowmelt~~snow disappearance timing and fire
2 ignitions across boreal North America

3 Thomas D. Hessilt¹, Brendan M. Rogers², Rebecca C. Scholten¹, Stefano Potter², Thomas A.J. Janssen¹
4 and Sander Veraverbeke¹

5 1 Faculty of Science, Vrije Universiteit Amsterdam, Amsterdam, The Netherlands

6 2 Woodwell Climate Research Center, Falmouth, MA, USA

7

8 **Correspondence:** Thomas D. Hessilt (t.d.hessilt@vu.nl)

9 Abstract

10 The snow cover extent across the Northern Hemisphere has diminished while ~~fire extent and severity~~the
11 number of lightning ignitions and burned area ~~have~~s increased over the last five decades with accelerated
12 warming. However, the effects of earlier ~~snowmelt~~snow disappearance on fire ~~is~~are largely unknown.
13 Here, we assessed the influence of ~~snowmelt~~snow disappearance timing on fire ignitions across 16
14 ecoregions of boreal North America. We found spatially divergent trends in earlier (later) ~~snowmelt~~snow
15 disappearance, which led to an increasing (decreasing) number of ignitions for the northwestern
16 (southeastern) ecoregions between 1980 and 2019. Similar northwest-southeast divergent trends were
17 observed in the changing length of the snow-free season and correspondingly the fire season length. We
18 observed increases (decreases) over Northwest (Southeast) boreal North America which coincided with a
19 continental dipole in air temperature changes between 2001 and 2019. Earlier ~~snowmelt~~snow
20 disappearance induced earlier ignitions of between 0.22 and 1.43 days earlier per day of earlier
21 ~~snowmelt~~snow disappearance in all ecoregions between 2001 to 2019. Early-season ignitions (defined by
22 the 20 % earliest fire ignitions per year) developed into significantly larger fires in 8 out of 16 ecoregions
23 ~~and, being on average~~ 77 % larger across the whole domain. Using a piecewise structural equation model,
24 we found that earlier ~~snowmelt~~snow disappearance is a good direct proxy for earlier ignitions but may
25 also result in a cascade of effects from earlier desiccation of fuels and favorable weather conditions that
26 led to earlier ignitions. This indicates that ~~snowmelt~~snow disappearance timing is an important trigger of
27 land-atmosphere dynamics. Future warming and consequent changes in ~~snowmelt~~snow disappearance
28 timing may contribute to further increases in western boreal fires while it remains unclear how the
29 number and timing of ~~fires~~fire ignitions in eastern boreal North America may ~~increase to~~change with
30 climate change.

31 1. Introduction

32 Snow cover across boreal and Arctic ecosystems is an important driver of regional hydrological cycles
33 and the global energy balance (Swenson and Lawrence, 2012; Li et al., 2017). With climate warming,

34 spring snow cover has decreased 11 % per decade over the Northern Hemisphere since 1970s (Déry and
35 Brown, 2007; Brown and Robinson, 2011). Changes in snow cover and sea ice have led to a substantial
36 decrease in the cryosphere radiative forcing across the Northern Hemisphere of around 0.5 W m^{-2} from
37 1979 to 2008, which warms the regional and global climate (Flanner et al., 2011; Groisman, et al., 1994).
38 This feedback ~~importantly~~ contributes to accelerated warming in the northern high latitudes (Anisimov et
39 al., 2007; Rantanen et al., 2022). ~~However, the changes in snow cover are heterogeneous across the~~
40 ~~Northern Hemisphere, .H~~owever, the changes in snow cover are heterogeneous across the Northern
41 hHemisphere (Bormann et al., 2018; Suzuki et al., 2020). Over boreal North America, changes in snow
42 cover timing show a long-term spatial divergence between earlier (later) ~~snowmelt~~snow disappearance
43 timing over western (eastern) boreal North America between 1972 and 2017 (Chen et al., 2016; Bormann
44 et al., 2018). The divergent changes in snow cover will likely have important impacts on ecosystem
45 functioning in boreal forest and Arctic tundra (Post et al., 2009; Buermann et al., 2013) and may
46 ~~potentially be attributed to~~drive be the result from persistent changes in atmospheric circulations (Jain and
47 Flannigan, 2021).

48 Simultaneously, over the last two decades, large parts of western boreal North America have
49 experienced a rise in the number of lightning fire ignitions and burned area, (Hanes et al., 2019), driven
50 by increases in dry fuel availability (Abatzoglou et al., 2016; Hessilt et al., 2022), favorable fire weather
51 (Sedano and Randerson, 2014), and increase in the number of lightning strikes (Veraverbeke et al., 2017).
52 Fire is the most widespread ecosystem disturbance ~~change~~ in boreal North America and these increasing
53 trends in fire occurrence are expected to continue in the future (Flannigan et al., 2005; Balshi et al., 2009;
54 Chen et al., 2021; Phillips et al., 2022). Early ~~snowmelt~~snow disappearance has previously been linked to
55 large fires in the western United States as a consequence of longer periods of fuel drying (Westerling et
56 al., 2006). Dry fuel availability is a prerequisite for fire ignitions (Abatzoglou et al., 2016; Hessilt et al.,
57 2022), and may further enable rapid fire growth thereby resulting in larger fires (Sedano and Randerson,
58 2014; Veraverbeke et al., 2017). The relationships between ~~snowmelt~~snow disappearance timing and fire

59 behavior characteristics, such as fire ignitions and size, may vary across boreal North America and remain
60 poorly understood: [\(Hanes et al., 2019\)](#).

61 In recent years, early [snowmelt/snow disappearance](#) after warm winters has been linked to
62 summer heatwaves and severe fire seasons over Siberia (Gloege et al., 2022; Scholten et al., 2022). Warm
63 winter extremes can substantially impact ecosystem functioning until deep into the subsequent growing
64 season (Zona et al., 2022). Early [snowmelt/snow disappearance](#) induces an early vegetation green-up
65 because of early peaks in soil moisture (Gloege et al., 2022) but a decreased late season vegetation
66 productivity (Buermann et al., 2013; Miles and Esau, 2016; Graham et al., 2017). The enhanced
67 evapotranspiration can lead to soil desiccation [in spring](#) and result in increased sensible heat flux later in
68 spring (Gloege et al., 2022). This enhances atmospheric warming and drying through limited evaporative
69 cooling (Seneviratne et al., 2010). In turn, positive geopotential height anomalies and persistent
70 atmospheric ridge [can](#) formations (Cohen et al., 2014; Tang et al., 2014) ~~that and~~ promote atmospheric
71 blocking events ~~thereby that~~ create favorable weather conditions for fire ignition and spread (Coumou et
72 al., 2018; Jain and Flannigan, 2021; Scholten et al., 2022). Simultaneously, destabilization of the
73 atmosphere increases the occurrence of convective thunderstorms and lightning (Chen et al., 2021), ~~and t.~~
74 [The increases in cloud-to-ground lightning strikes can potentially increase](#) the likelihood of igniting
75 dry fuels (Hessilt et al., 2022). Nonetheless, the influence of a divergent snow cover trend across boreal
76 North America on weather, fuel dryness, and ignition timing has previously not been studied and may
77 exhibit divergent responses to changes in the snow cover.

78 Earlier [snowmelt/snow disappearance](#) may also lead to an earlier start of the fire season ~~and~~
79 ~~possibly more severe fire weather~~, thereby lengthening and intensifying the boreal fire season (~~Flannigan~~
80 ~~et al., 2005; Veraverbeke et al., 2017~~)([Flannigan et al., 2005; Bartsch et al., 2009; Veraverbeke et al.,](#)
81 [2017](#)). [Defining the fire season length is not straightforward and](#) different methods have been used to
82 quantify the length of the boreal fire season. The fire season length has been estimated using fire weather
83 indices as proxies of fire activity (Wotton and Flannigan, 1993; Flannigan et al., 2016). Other studies

84 have estimated the fire season length using long-term government records, which are prone to temporal
85 changes in accuracy and uncertainties (Hanes et al., 2019). Daily fire monitoring using the polar-orbiting
86 Moderate Resolution Imaging Spectroradiometer (MODIS) sensors allows accurate definition of the fire
87 season based on observed fire activity since the 2000s (Justice et al., 2002; Giglio et al., 2016, 2018).
88 Given that the MODIS record dates back until the early 2000s, it may be possible to infer changes in fire
89 season length across boreal North America during this period.

90 Here, we investigated relationships between snowmeltsnow disappearance and early season
91 ignition timing across boreal North America between 2001 and 2019. In addition, we evaluated the
92 influence of ignition timing on fire size and assessed temporal changes in snowmeltsnow disappearance
93 timing and the number of ignitions since 1980. Through satellite-derived estimates, we derived the length
94 of the snow-free and the fire seasons, and assessed the influence of the length of the snow-free season on
95 fire season length. Early ignition timing was modeled as a function of snowmeltsnow disappearance
96 timing, and meteorological and fire weather conditions using a linear mixed-effect model to investigate
97 potential cascading effect of earlier snowmeltsnow disappearance timing. Finally, we assessed the
98 interactions between snowmeltsnow disappearance timing, and meteorological and fire weather
99 conditions when modeling ignition timing through a piecewise structural equation model.

100

101 **2. Methodology**

102 *2.1 Study domain*

103 The study domain includes Alaska, USA, and the majority of Canada (9.17×10^6 km²) excluding the
104 Canadian Arctic Archipelago, and is divided into sixteen ecoregions (Omernik, 1987, 1995) (Fig. 1). We
105 used the second-level ecoregions for subcontinental comparisons (McCoy and Neumark-Gaudet, 2022).
106 We included 14 ecoregions but further divided the Softwood Shield and Taiga Shield into eastern and
107 western ecoregions due to their large longitudinal gradients, resulting in 16 different ecoregions in our

108 study (Fig. 1 and Table S1). The Softwood Shield was divided in accordance with the third-level
109 ecoregion division and the Taiga Shield was split into two sub-regions East and West of Hudson Bay
110 (Baltzer et al., 2021) (Fig. 1). The northernmost ecoregions (the Arctic Cordillera, Northern Arctic, and
111 Southern Arctic) were excluded as they included very few ignitions. The southern parts of the Cold
112 Deserts, Marine West Coast Forest, Mixed Wood Shield, and Western Cordillera were cropped out as
113 they were not covered by the Arctic-Boreal Vulnerability Experiment Fire Emission Database (ABOVE-
114 FED; Potter et al., 2023) extent (Fig. 1). Our study domain thus included Arctic tundra ~~and~~ boreal forest,
115 ~~and temperate~~ ecosystems between Northwest Alaska and Southeast Canada, hereafter referred to as
116 “boreal North America”.

117

118 2.2 ~~Snowmelt~~ Snow disappearance timing

119 We retrieved ~~snowmelt~~ snow disappearance timing at 463 m resolution from the MODIS daily composite
120 snow-cover product MOD10A1 collection 6 between 2001 to 2019 (Hall and Riggs, 2016). This product
121 computes the normalized difference snow index (NDSI) ranging from ~~-10~~ to 1 from visible and shortwave
122 infrared spectral data. The relationship between NDSI and estimated fractional snow cover from higher
123 resolution snow cover data from Landsat Enhanced Thematic Mapper-plus (30 m) has previously been
124 proven robust over large areas such as boreal North America (Salomonson and Appel, 2004). This
125 allowed us to use NDSI as a proxy for fractional snow cover. We identified the Julian calendar day of
126 ~~snowmelt~~ snow disappearance timing as the first day a pixel had less than or equal to 15 % snow cover for
127 a minimum of 14 consecutive days (Verbyla, 2017). We also tested a threshold of snow cover less than or
128 equal to 15 % for a minimum of seven consecutive days, but found little difference between the two
129 thresholds (Fig. S1, Table S2). Pixels that had burned or contained persistent cloud cover, water, or
130 perennial snow cover (more than 250 days a year), or less or equal than 15 % snow cover for less than 14
131 consecutive days were excluded from the analysis. Pixels that contained persistent cloud cover, water, or
132 perennial snow cover (more than 250 days a year), or less or equal than 15 % snow cover for less than 14

133 ~~consecutive days were excluded from the analysis.~~ As pPixels with values exceeding a pixel-specific
134 threshold (average ~~snowmelt~~snow disappearance timing in 2001-2019 \pm 3 standard deviations) were
135 regarded as outliers and excluded from the analysis. The ~~snowmelt~~snow disappearance timing was
136 determined between February 1 and July 31. We opted for a large potential range in ~~snowmelt~~snow
137 ~~disappearance~~ timing because of the large latitudinal and thus climatological range present in the study
138 domain (Fig. 1). To retrieve the first day of snow cover, we used the reversed method where the first day
139 on which at least 15 % of the pixel was snow covered for a minimum of 14 consecutive days was set to
140 first day of snow cover. This was determined between August 1 and December 31. We modified the code
141 from Armstrong et al. (2023) to compute the ~~snowmelt~~snow disappearance timing in Google Earth
142 Engine.

143 In complement to the MODIS snow cover product, we also used the Northern Hemisphere Equal-
144 Area Scalable Earth Grid 2.0 version 4 weekly snow cover product (NSIDC) to calculate long-term
145 ~~snowmelt~~snow disappearance timing and snow cover onset trends since 1980 (Brodzik and Armstrong,
146 2013; Estilow et al., 2015). The NSIDC product is based on the National Oceanic and Atmospheric
147 Administration (NOAA) climate data record (Robinson et al., 2012). It uses visual interpretation of snow
148 cover detected from a range of sensors (i.e. Advanced Very High Resolution Radiometer (AVHRR),
149 Geostationary Operational Environmental Satellite (GOES), and more recently MODIS (Helfrich et al.,
150 2007)) and interpolated to the Equal-Area Scalable Earth (EASE) ~~grid with 25 km spatial resolution.~~grid
151 ~~of 25 km.~~ The NSIDC product is influenced by image availability and user interpretation of images
152 (Ramsay, 1998; Helfrich et al., 2007). It uses a binary indication of snow or no snow cover. We therefore
153 computed the annual first day with no snow cover for all pixels. Similar to the MODIS product, the
154 ~~snowmelt~~snow disappearance timing was determined between February 1 and July 31. The MODIS and
155 NSIDC snow cover products differ both in their temporal and spatial resolutions, but we found reasonable
156 agreement between ~~snowmelt~~snow disappearance timing from both products across the study domain
157 (RMSE = 12.57 Julian day, $r = 0.76$ $p < 0.01$) and individual ecoregions (Fig. ~~S1S2~~).

158

159 2.3 Fire information

160 The location and timing of the fire ignitions, and their associated burned area, were derived from the
161 Arctic-Boreal Vulnerability Experiment Fire Emission Database (ABOVE-FED) product (Potter et al.,
162 2023). The ABOVE-FED burned area product covers Alaska and Canada (2001-2019) and is derived from
163 thresholding the differenced normalized burn ratio (dNBR) from Landsat imagery at 30 m resolution
164 complemented by MODIS surface reflectance products at 500 m resolution (MOD09GA and MYD09GY
165 v6) when no Landsat data were available. The dNBR thresholding within the ABOVE-FED product was
166 limited to the fire perimeters from the Alaskan Large Fire Database (ALFD, (Kasischke et al., 2002)) and
167 Canadian Large National Fire Databases (~~CLFD~~CNFDB, (Stocks et al., 2002)) and MODIS active fire
168 locations, and their surroundings, to minimize commission errors from non-fire disturbances
169 (Veraverbeke et al., 2015; Potter et al., 2023).

170 The retrieval of ignition timing and location was adapted from Scholten et al. (2021b). This
171 algorithm uses the spatiotemporal information in the ABOVE-FED burned area product to delineate
172 individual fire perimeters and a minimum search radius to detect the location of each unique ignition
173 spatially and temporally. Since burned area pixels in boreal regions can be discontinuous due to varying
174 fire severity and possibly omitted pixels, we applied different buffers (1 km and 2 km) to group the fire
175 pixels into fire perimeters. Several combinations of the fire perimeter buffers (1 km and 2 km), search
176 radii (5 km, 7.5 km, 10 km, and 15 km), and minimum fire sizes (i.e., exclusion of fires from 1 or 2
177 individual burned pixels) were examined to minimize the commission and omission errors. We tested
178 these three fire size thresholds, as single or double pixel burned area could be small anthropogenic fires or
179 commission errors. We compared the results to the ignitions present in the Alaskan Fire Emission
180 Database (AKFED) version 2 (Scholten et al., 2021a) (Table ~~S2S~~S3). We used ignition locations and
181 timing retrieved inside 2 km buffered fire perimeters, using a 7.5 km search radius for fires larger than 50
182 ha (1 and 2 pixel fires removed) as this was in good agreement with the AKFED-derived ignitions (Table

183 ~~S2S3~~). This led to an exclusion of 15 % ignition locations compared to an inclusion of all fire sizes. In
184 Alaska, Yukon, and the Canadian Northwest Territories, we found approximately 6 % more ignitions in
185 ABoVE-FED compared to AKFED, and 76 % overlap between the two ignition datasets.

186 For this study, we also removed ignition locations that were not covered by snow between 2001
187 and 2019 and ignitions that were erroneously detected before ~~snowmelt~~snow disappearance
188 (approximately 11 % of the observations). For the whole study domain and period, we analyzed a total of
189 17 957 ignitions (Fig. 1b). When possible, we assigned the ignition cause, lightning or anthropogenic,
190 from the ignition cause attribute of the ALFD and ~~CLFDCNFDB~~ when ignitions fell within the fire
191 perimeter from the same year. By doing so, 4 % of the ignitions were attributed an anthropogenic cause,
192 38 % were attributed a lightning cause, and the cause of the remaining 58 % was unknown. The daily
193 timing and exact location of fire ignitions were derived from the ABoVE-FED data between 2001 and
194 2019, but we extended the number of ignitions within ecoregions back to 1980 using fire perimeter data
195 from the ALFD and ~~CLFDCNFDB~~. The start year 1980 was chosen as it corresponds to major
196 optimization of lightning detection systems for Canada that minimized erroneous attribution of causes to
197 fires (Stocks et al., 2002).

198 We established a relationship between the number of ignitions from ABoVE-FED and the
199 number of fire perimeters from the ALFD and ~~CLFDCNFDB~~ for the overlapping period between 2001
200 and 2019 per ecoregion (Fig. ~~S2S3~~). The ~~statistical relationship~~linear regression between the number of
201 ignitions and fire perimeters was forced through the origin as no fire perimeter can occur without an
202 ignition and vice versa (Fig. ~~S2S3~~). The minimum mapping unit (MMU) was 200 ha in ~~CLFDCNFDB~~
203 before 1997 (Stocks et al., 2002), and 405 ha in ALFD before 1988 (French et al., 2015). To minimize
204 uncertainties because of recent changes in the mapping accuracy, we removed fires smaller than 200 ha
205 from the ~~CLFDCNFDB~~ and fires smaller than 405 ha from the ALFD similar as in Scholten et al. (2021b)
206 and Veraverbeke et al. (2017). Similarly, ABoVE-FED fires smaller than MMUs were excluded when
207 developing these relationships. We used the established statistical relationship between ignitions and fire

208 perimeters in each ecoregion from 2001 to 2019 to estimate the annual numbers of ignitions between
209 1980 and 2000.

210

211 *2.4 Influence of snowmelt snow disappearance timing on ignition timing and fire size*

212 For each ignition location, we retrieved the snowmelt snow disappearance timing by averaging the
213 MODIS-derived day of snowmelt snow disappearance timing over each ignition location, including its
214 spatial uncertainty derived from the ignition algorithm. Snowmelt snow disappearance timing may be an
215 important modulator of fire ignitions in the early fire season, whereas seasonal soil moisture dynamics
216 may more importantly influence fire behavior later in the fire season (Flannigan et al., 2016; Gergel et al.,
217 2017). To evaluate the relationship between snowmelt snow disappearance and ignition timing between
218 2001 and 2019, we focused on ignitions that occurred early in the fire season. To define early fire season
219 ignitions, we first evaluated the correlation between the annual snowmelt snow disappearance timing and
220 ignition timing for all ignitions, per ecoregion. We then re-evaluated these relationships by only including
221 a fraction of the ignitions. This fraction was derived from taking a percentile of the ignition timing
222 distribution, between the first and 99th percentile. We generally found significant positive correlations
223 between snowmelt snow disappearance timing and ignition timing for all percentiles with a general
224 decline in correlation strength with inclusion of ignitions later in the fire season (Fig. S3S4). Thus, we set
225 the ignition timing threshold to the annual 20th percentile of the ignition timing distribution; to account for
226 potential interannual differences in weather and snow disappearance timing interfering with the ignition
227 timing. For this threshold, all ecoregions showed strong significant Pearson r correlation (range: 0.25 to
228 0.77) between snowmelt snow disappearance and ignition timing (Fig. S3S4). By doing so, we retained 3
229 849 ignitions that occurred between the Julian days 58 and 294 across the study domain (Fig. S4S5).

230 We also compared all early- versus late-season ignitions to examine the importance of ignition
231 timing on fire size. The burned area caused by an ignition was assigned to the given day of the ignition. In
232 case of multiple ignition locations detected for one fire perimeter (approximately 4 % of the perimeters),

233 the burned area was assigned to the earliest ignition ~~day of the year~~. We summed up the total burned area
234 between 2001 and 2019 per ignition day. The threshold between early and late ignition timing was again
235 set as the annual 20th percentile day of ignition timing per ecoregion.

236

237 2.5 Climatic drivers of ~~snowmelt~~snow disappearance and ignition timing

238 The meteorological drivers of ~~snowmelt~~snow disappearance timing and ignition timing were assessed
239 with hourly meteorological data derived from the fifth generation of the European Centre for Medium-
240 Range Weather Forecast's (ECMWF) reanalysis for the climate and weather (ERA5 reanalysis) at 0.25°
241 resolution (Hersbach et al., 2020). ERA5 reanalysis data have been used before in other studies that
242 investigated extreme weather events and fires in the northern high latitudes (Gloege et al., 2022; Parisien
243 et al., 2023). Furthermore, several of the ERA5 variables, such as precipitation, surface temperature, and
244 specific humidity have been validated with ground observations over the study region (Alves et al., 2020).
245 Fire weather data were collected from the Global ECMWF Fire Forecast ERA5 reanalysis dataset (GEFF-
246 ERA5) of fire danger at 0.25° resolution (Vitolo et al., 2020). We extracted convective potential available
247 energy (CAPE), total precipitation, precipitation type (rain vs. snow), air temperature at 2 m, and
248 dewpoint temperature at 2 m from the ERA5 reanalysis. From these variables we further derived relative
249 humidity and vapor pressure deficit (VPD) (Table S3S4). The fine fuel moisture code (FFMC), duff
250 moisture code (DMC), and drought code (DC) were collected from GEFF-ERA5 and are designed to
251 represent the fuel moisture of the top (1-2 cm organic layer, lag-time of 2/3 of a day), intermediate (5-10
252 cm sub-organic layer, lag-time of 12 days) and deep (15-20 cm deep organic layer, lag-time of 52 days)
253 soil layers (Van Wagner, 1987). In regions regularly covered by snow, all fuel load variables are initiated
254 on the third day after the snow has melted while in regions without snow cover, calculations begin on the
255 third consecutive day with noon air temperatures of < 12 °C (Lawson and Armitage, 2008). Here, we used
256 the fire weather variables as proxies for fuel dryness.

257 We calculated spatially explicit daily anomalies for all meteorological and fire weather variables
258 by subtracting the climatic daily averages between 1980 and 2019 from the daily observations between
259 2001 and 2019. We assessed the effect of precipitation, precipitation type (rain vs. snow), air temperature,
260 and relative humidity on snowmeltsnow disappearance timing. Precipitation, air temperature, and relative
261 humidity anomalies were averaged for the 30 days leading up to the day of snowmeltsnow disappearance
262 timing. The number of days with snowfall, rainfall, and no precipitation were summed up for the 30 days
263 leading up to the day of snowmeltsnow disappearance timing. The averages of all weather and fire
264 weather anomalies, excluding precipitation type, between the day of snowmeltsnow disappearance timing
265 and ignition timing were used to assess their influence on ignition timing.

266

267 *2.6 Temporal trends in snow-free season and fire season*

268 The temporal trends in the snow-free and fire season lengths were analyzed between 2001 and 2019. The
269 snow-free season length was calculated by subtracting the ecoregion average day of snowmeltsnow
270 disappearance timing from the ecoregion average day of snowmeltsnow disappearance offset for each
271 year from the MODIS product.

272 We evaluated several scenarios to define the fire season timing. For the fire season start, we
273 assessed scenarios between the day of the first ignition and the 20th percentile of the ignition timing
274 distribution. For the fire season end, we assessed scenarios between-of the day during-whichwhere 80 to
275 99 % of the annual burned area had occurred. First, we analyzed the percentage of annual burned area that
276 was excluded for different fire season start and ending scenarios (Fig. S5S6). We performed a sensitivity
277 analysis of the different cut-off values that showed no substantial changes in the relationship between the
278 length of the snow free period and the fire season length (Fig. S6S7). After evaluation, we chose the 1st
279 percentile day of ignition as fire season start and the day on which 99 percent of the annual burned area
280 had occurred as fire season end day. We subtracted the first day of ignition timing from the day of the 99th

281 percentile total burned area each year to calculate the fire season length. We also investigated changes in
282 the snow-free season length in relation to fire season length between 2001 and 2019.

283

284 *2.7 Statistical analysis*

285 All statistical analyses were performed in R statistical software version 4.2 (R Core Team, 2022). We
286 investigated temporal trends between 1980 and 2019 and between 2001 and 2019 in snowmeltsnow
287 disappearance timing ~~and~~and the number of ignitions using simple linear regression. The snow-free
288 season length and fire season length in each ecoregion were analyzed between 2001 and 2019 using
289 simple linear regression. The statistical difference in the average fire size between early and late ignitions
290 was analyzed with a Wilcoxon-Mann-Whitney rank sum test (Mann and Whitney, 1947). We
291 distinguished between two significance levels of $p < 0.05$ and $p < 0.1$.

292 To assess the ecoregional drivers of the divergent snowmeltsnow disappearance timing and early-
293 season ignition timing, defined as the annual 20th percentile ignitions, we used a linear mixed effect
294 model. Prior to testing, ignition locations in close proximity were spatially correlated (Moran's I = 0.30).
295 We therefore averaged all ignitions for each ecoregion per year to reduce the spatial autocorrelation. The
296 snowmeltsnow disappearance was modeled as a function of weather while the ignition timing was
297 modeled as functions of weather and fire weather independently. This was to minimize the multi-
298 collinearity in the generalized linear mixed-effect models. We conducted our linear mixed-effect models
299 with ecoregions (16 levels) as random effects using the 'nlme' package (Pinheiro et al., 2022) (Tables
300 S4S5 and S5S6) (eq. 1) to account for additional temporal and spatial autocorrelation. We excluded year
301 as random effect as it only explained around 3% and 7% of the variation in snowmeltsnow disappearance
302 and ignition timing, respectively. We conducted three linear mixed-effect models for all ecoregions
303 combined ($n = 299$), ecoregions with earlier snowmeltsnow disappearance timing trends ($n = 186$) and
304 later snowmeltsnow disappearance timing trends ($n = 113$) based on the MODIS-derived snowmeltsnow
305 disappearance timing (Table S1):

306
$$y = X\beta + Zu + \varepsilon$$

307 (1)

308 where y is the response variable, $X\beta$ represents the fixed effects, where X is a matrix of observed values
309 per variable and β represents the regression coefficient for each variable. The Zu term represents the
310 random effects, where Z is a matrix for observed values per covariate of random effects and u is the
311 random effect of the covariates. The error term ε represents the residuals.

312 All variables were standardized prior to testing and the analysis was conducted for ignitions
313 between 2001 and 2019. The significance of the fixed effects was tested using likelihood ratio tests of the
314 reduced and full models. We used the Akaike information criterion (AIC) to verify the significance of the
315 models compared to reduced models (Zuur et al., 2009). The best model fit was chosen to be the linear-
316 mixed model with different intercepts per random effect (ecoregion) but similar slopes for every predictor
317 and random effect. For further variable selection for our piecewise Structural Equation Model (pSEM),
318 we evaluated the influence of meteorological variables (Table S6S7) on the day of snowmeltsnow
319 disappearance timing and the additional influence of snowmeltsnow disappearance timing and the fuel
320 codes on ignition timing through a redundancy analysis in the R package ‘vegan’ (Oksanen et al., 2013)
321 (Table S6S7). The significance of the unique contribution of all drivers included in the two variance
322 partitioning analyses was determined by adjusted R^2 and $p < 0.05$. The shared variance and the residual
323 variance between drivers were also computed (Table S6S7).

324 We expected that the interactions between predictor variables and the snowmeltsnow
325 disappearance and ignition timing constituted a complex network and therefore deployed a pSEM in the
326 package ‘piecewiseSEM’ (Lefcheck, 2016). The pSEM creates a single causal network from our deployed
327 multiple linear-mixed effect models that incorporates a random structure (Shipley, 2009). We included
328 explanatory variables linked to snowmeltsnow disappearance and ignition timing based on analysis of
329 bivariate relationships of meteorological and fire weather data that could influence the timing of
330 snowmeltsnow disappearance and ignition. Bivariate relationships were evaluated by simple linear

331 regressions between snowmeltsnow disappearance timing and the respective predictor variables, and
332 ignition timing at its potential explanatory variables (Table S7S8). The hypothesized network of
333 interactions in our pSEM was modelled for three individual pSEMs to test this hypothesized model of
334 interaction between weather, fire weather and snowmeltsnow disappearance timing but also to describe
335 the potential effect of divergent snowmeltsnow disappearance timing across the study domain. We
336 modelled a pSEM: (1) for all ecoregions, (2) ecoregions with early snowmeltsnow disappearance timing
337 trends in accordance with the MODIS trend analysis (Table S1), and (3) ecoregions with later
338 snowmeltsnow disappearance timing trends in accordance with the MODIS trend analysis (Table S1).

339 For modelling snowmeltsnow disappearance timing, we hypothesized that, (1) as the total amount
340 of precipitation decreases and the air at the surface becomes drier, increased surface air temperature
341 would accelerate snowmeltsnow disappearance timing. We also hypothesized that, (2) snowmeltsnow
342 disappearance timing would occur earlier with increased days of no precipitation (smaller snowpack) or
343 days with rain-on-snow events (more rainfall) compared to snow-on-snow events (more snowfall). We
344 hypothesized that, (3) earlier snowmeltsnow disappearance timing would result in earlier ignition timing.
345 For modelling the influence of snowmeltsnow disappearance timing on weather and fire weather
346 variables, we hypothesized that, (4) surface relative humidity and precipitation would decrease and limit
347 the evaporative cooling and in turn result in higher air temperatures. This would increase atmospheric
348 instability and the CAPE and would all increase the likelihood of earlier ignitions. Lastly, we
349 hypothesized that (5) earlier snowmeltsnow disappearance timing would promote drying of fuels (FFMC,
350 DMC, and DC) more pronouncedly in ecoregions with earlier snowmeltsnow disappearance timing. We
351 allow for links between weather and fire weather variables, since DC, DMC, and FFMC are derived from
352 precipitation, relative humidity and air temperature while the calculation of FFMC also ingested wind
353 speed. These interactions are included to comply to statistical requirements of inclusion of missing paths
354 in the pSEM analysis but left out of the figure for simplicity reasons (Fig. S7). ~~As the pSEMs can consist~~
355 ~~of many different linear models, we fitted each component of the pSEM with a linear mixed effect~~

356 ~~model-S8~~). We also substituted relative humidity and air temperature for vapor pressure deficit in similar
 357 pSEMs as #VPD has been shown to substantially influence fire ignition and spread (Fig. S9) ~~substantially~~
 358 (Sedano and Randerson, 2014; Veraverbeke et al., 2017). As the pSEMs can consist of many different
 359 linear models, we fitted each component of the pSEM with a linear mixed-effect model. Therefore, the
 360 influence of fire weather and weather on ignition timing were modelled separately. We included the
 361 influence of snow disappearance timing in the model that contained weather variables predicting ignition
 362 timing. We assessed potential additional variable interaction and their conditional independence using
 363 Shipley's test of dependence separation (*d*-sep). The test is founded on the χ^2 distributed and combines
 364 the Fisher's C statistics with $2j$ degrees of freedom, where j is the number of independent interactions in a
 365 basis set (Shipley, 2009) (eq. 2):

$$C = -2 \sum_{i=1}^k \ln(p_i) \tag{2}$$

367 where k is the number of independence claims, p_i is the null probability of the independence test
 368 associated with the i^{th} independence claim.

370 The missing paths determined by the *d*-sep test were included in the hypothesized pSEM to accurately
 371 analyze the network of dependent variables in our overall pSEM. The global goodness-of-fit of our
 372 models and the hypothesized model was evaluated by the *d*-sep. With p -values > 0.05 , the representative
 373 model misses no paths and is in accordance with the hypothesized model (Shipley, 2009). The estimates
 374 of paths from predictor variables to response variables for each pSEM were standardized for comparison
 375 of effects across multiple responses and their indirect and total effects. The standardization of coefficients
 376 was done by the ratio of the standard deviation of the independent and dependent variable of the given
 377 variables (eq. 3):

$$\beta_{std} = \beta \times \left(\frac{sd_x}{sd_y} \right)$$

379

(3)

380 , where β is the unstandardized coefficient, sd_x is the standard deviation of the independent variable, and
381 sd_y is the standard deviation of the dependent variable. The explained variation of snowmeltsnow
382 disappearance and ignition timing from the different components in the pSEMs were analyzed using the
383 marginal and conditional R^2 . Marginal R^2 represents the variation explained only by the fixed effects, and
384 conditional R^2 shows the variation explained by a combination of fixed and random effects.

385

386 3. Results

387 3.1 Trends in snowmeltsnow disappearance timing and ignitions

388 The long-term (1980-2019) and short-term (2001-2019) snowmeltsnow disappearance timing trends over
389 boreal North America showed somewhat similar patterns. Long-term snowmeltsnow disappearance
390 timing trends ~~occurred~~demonstrated shifts towards earlier ~~in the northern~~snow disappearance timing in 13
391 out of 16 ecoregions, ~~however more pronounced~~but this trend was only significant in three ecoregions (p
392 < 0.05) (Fig. 2a). ~~These significant trends towards earlier snow disappearance were observed in~~
393 ~~Northwestern boreal North America,~~with only interior ecoregions (Fig. 2b A-D) while three southern
394 ecoregions ~~showing~~(Boreal Plain, Mixed Wood Shield, and Eastern Softwood Shield) showed later
395 snowmeltsnow disappearance timing between 1980 and 2019 (Fig. 2a M, O, P). ~~Between 2001 and 2019,~~
396 ~~this~~2a). The spatial divergence, ~~however,~~promoted to in the trends of snow disappearance timing has
397 developed into a distinct west-east divergence ~~in the snowmelt timing trend~~ across boreal North America.
398 ~~We observed,~~with increasingly earlier snowmeltsnow disappearance observed in western boreal North
399 America versus later snowmeltsnow disappearance in the eastern ecoregions with only four ecoregions
400 showing statistically significant changes ($p < 0.05$) between 2001 and 2019. ~~This trend has also become~~
401 ~~more pronounced in the last two decades~~ (Figs. 1a and 2, and Table S1). The west-east divergence in
402 snowmeltsnow disappearance timing ranged from advances of up to 11 days per decade in the western
403 ecoregions to delays of up to 8 days per decade in the eastern part of the study region in the MODIS era

404 (2001-2019). The long-term NSIDC snow product (1980-2019) showed trends between advances in
405 snowmeltsnow disappearance timing of 3 days per decade in the west to delays of 2 days per decade in
406 the East (Table S1). On average, snowmeltsnow disappearance advanced 1.6 (standard deviation: 0.7)
407 days per decade ($p < 0.05$) in the western ecoregions (Fig. 2 A-H, J, L), while snowmeltsnow
408 disappearance occurred 1.8 (standard deviation: 0.9) days per decade later in the central and eastern
409 ecoregions ($p = 0.05$) (Fig. 2 I, K, M-P). We observed the most pronounced earlier snowmeltsnow
410 disappearance trends of 2.1 (standard deviation: 0.5) days earlier snowmeltsnow disappearance per
411 decade ($p < 0.05$) in northwestern ecoregions (Fig. 2 A-E), while the most pronounced later
412 snowmeltsnow disappearance trends mainly occurred in the southern ecoregions of 1.1 (standard
413 deviation: 0.8) days per decade ($p = 0.05$) (Fig. 2 M-P). The spatially diverging trends in snowmeltsnow
414 disappearance timing are associated with similar trends in early spring (February-April) air temperature
415 between 1980 and 2019 (Fig. S8aS10a). The northernmost ecoregions showed the largest increase in early
416 spring air temperature, while the southern ecoregions experienced decreasing early spring air temperature
417 over the last four decades. Superimposed on this north-south gradient, we also found that the west of the
418 study domain experienced pronounced early spring warming while the east of the study domain
419 experienced early spring cooling (Fig. S8S10). The distinct spatial divergence in short-term
420 snowmeltsnow disappearance timing trends also follows a more pronounced short-term early spring air
421 temperature dipole. Early spring ~~time~~-air temperatures increased with up to 3.5°C over western ecoregions
422 with earlier snowmeltsnow disappearance timing trends and decreased with up to 2.1°C over southeastern
423 ecoregions showing delayed snowmeltsnow disappearance timing (2001-2019) (Fig. S8bS10b).

424 In accordance with the spatial diverging trends in snowmeltsnow disappearance timing and early
425 spring air temperatures, the trends in the number of ignitions also showed a west-east divergence. The
426 northwestern ecoregions that displayed a pronounced earlier snowmeltsnow disappearance also exhibited
427 an increase in the total number of ~~total~~-ignitions of 0.9×10^{-6} (standard deviation: 0.8×10^{-6}) $\text{km}^{-2} \text{decade}^{-1}$
428 ($p < 0.05$) (Fig. 2 A-G) between 1980 and 2019. The southwestern ecoregions of the Cold Deserts,

429 Marine West Coast Forest, and Western Cordillera demonstrated the strongest increasing trends in
430 ignitions (6.4×10^{-6} , standard deviation: 4.4×10^{-6} ignitions $\text{km}^{-2} \text{decade}^{-1}$, $p < 0.05$) (Fig. 2 H, J, L), while
431 the central and eastern ecoregions showed an overall decrease of 0.2×10^{-6} (standard deviation: 0.3×10^{-6})
432 ignitions $\text{km}^{-2} \text{decade}^{-1}$ ($p = 0.51$) (Fig. 2 I, K, M-P). However, there was no spatially divergent trend in
433 the temporal changes in ignition timing between 2001 and 2019. In 12 out of 16 ecoregions, there was a
434 shift towards earlier ignitions, when we included all ignitions, with 7 ecoregions showing significantly
435 earlier ignitions ($p < 0.1$). The trends towards earlier ignition ranged between 0.4 and 25 days per decade
436 (Table S1). Of the four ecoregions that showed later ignition timing trends, three were located in the
437 southwest of the study domain (Boreal Plain, Cold Deserts, and Western Cordillera), while the Western
438 Taiga Shield was the only northern ecoregion with-that showed a later ignition timing (Fig. S9S11 and
439 Table S1).

440

441 *3.2 Relationships between snowmelt snow disappearance and ignition timing*

442 In all ecoregions, we found significant positive relationships between snowmelt snow disappearance and
443 ignition timing in the early fire season (20th percentile of the ignition timing distribution) between 2001
444 and 2019 ($p < 0.1$) (Fig. 3). The strength of the relationships was similar across boreal North America and
445 the advance in ignition timing ranged between 0.22 and 1.43 days per day of earlier snowmelt snow
446 disappearance (Fig. 3). Ignitions occurred later and in a narrower temporal window in the northern
447 ecoregions (Fig. 3 A-I, K) and Eastern Softwood Shield (Fig. 3 P) compared to the other southern
448 ecoregions. Southern ecoregions also showed a more variable ignition timing at the beginning of the fire
449 season (Fig. 3 J, L-P). Furthermore, the southwestern ecoregions of our study domain showed a bimodal
450 ignition timing distribution, which could point to differences in ignition cause. Anthropogenic ignitions
451 dominate earlier in the fire season while lightning ignition are more prevalent around the summer solstice
452 (Fig. 3 J, L). Nonetheless, when we separated the anthropogenic and lightning ignitions, and ignitions

453 with unknown cause, we still observed positive relationships between [snowmelt](#)[snow disappearance](#) and
454 ignition timing for all causes (Table [S8S9](#)).

455

456 *3.3 Trends in snow-free and fire season lengths*

457 The temporal changes in the snow-free season length and the fire season length also showed a distinct
458 west-east divergence. Corresponding to the overall trends in the [snowmelt](#)[snow disappearance](#) timing, we
459 found that the northwestern ecoregions that show increasingly earlier [snowmelt](#)[snow disappearance](#) also
460 experience a prolonged snow-free season of 7.1 (standard deviation: 4.2) days per decade ($p < 0.1$) (Figs.
461 2a A-H, J, L and 4a A-H, J, L) between 2001 and 2019. The southeastern ecoregions where
462 [snowmelt](#)[snow disappearance](#) was ~~increasingly~~-occurring later in spring [also](#) exhibited a shortening of the
463 snow-free season of 7.3 (standard deviation: 4.7) days per decade (Figs. 2a I, K, M-P and 4a I, K, M-P),
464 however not significant ($p = 0.12$), between 2001 and 2019. The positive trend in snow-free season length
465 was significant in 5 of the 16 ecoregions, while only the Eastern Taiga Shield showed significant
466 shortening trend in snow-free season length between 2001 and 2019 ($p < 0.1$) (Table [S9S10](#)). We
467 observed similar spatial divergence in the long-term trends in changes in the snow-free season length
468 between 1980 and 2019 (Fig. [S10S12](#)).

469 The temporal changes in fire season length showed a west-east gradient in complement to a
470 north-south gradient for our study domain (Fig. 4b). The fire season length between 2001 and 2019
471 increased substantially from 1.7 and up to 25.3 days per decade and on average 5.8 (standard deviation:
472 7.6) days per decade for the northern ecoregions except in Taiga Plain (Fig. 4b A-H, K and Table [S9S10](#))
473 ($p = 0.45$). The southern ecoregions experienced an average shortening of the fire season length between
474 2001 and 2019 of 18.2 (standard deviation: 10.5) days per decade (Fig. 4b, I, J, L, M-O) ($p < 0.1$). The
475 northernmost ecoregions in our study region have experienced the largest prolonging of the fire season
476 over the last two decades of 18.0 (standard deviation: 10.1) days per decade (Fig. 4b, B, C, G) ($p < 0.1$).

477 We found that the snow-free season and fire season lengths between 2001 and 2019 were highly
478 correlated (Fig. 4c). There was a consistent significant positive relationship between the snow-free season
479 and fire seasons lengths across boreal North America between 2001 and 2019 regardless of the thresholds
480 set for the fire season start and end (Fig. ~~S5S76~~). Across the study domain, we observed a lengthening of
481 the fire season of 1.7 days for every day of prolonged snow-free season. The length of both the snow-free
482 season and the fire season was shortest in the northern ecoregions and gradually prolonged for more
483 southern ecoregions (Fig. 4bc). We also found that the trends in snow-free and fire season length
484 ~~tended~~ to correlate positively with each other with a prolonging of the fire season of 0.9 days per
485 decade for every day per decade increase in the snow-free season ($p < 0.05$) (Fig. = 0.08). ~~There was with~~
486 ~~large variation between ecoregions and (the trends in snow-free season lengths explained 45 % of the~~
487 ~~variation in the trends in fire season length) (Fig. 4d).~~

488

489 3.4 Ignition timing and fire size

490 ~~Early season~~Fire ignitions ~~that occurred in the early fire season (20th percentile earliest ignitions)~~ resulted
491 in ~~significantly~~-larger fires ~~than late-compared to fires that were ignited later in the season ignitions(80th~~
492 ~~percentile latest ignitions) in all ecoregions but the Alaska Tundra (Fig. 5 B) and the Eastern Softwood~~
493 ~~Shield (Fig. 5 P). This difference was significant~~ in 8 out of the 16 ecoregions ~~(at $p < 0.1$)-(Fig. 5). Only~~
494 ~~in two ecoregions, Alaska Tundra and Eastern Softwood Shield, late season fires on average grew larger~~
495 ~~compared to early season with the early ignited~~ fires ($p = 0.58$ and $p = 0.76$, respectively) (Fig. 5 B,P).
496 ~~resulting in 77 % larger fires compared to fires ignited later in the season across the study domain (Fig.~~
497 ~~5). On average,an~~ ecoregional ~~level, the~~ early ~~season~~ignited fires grew between 30 and 600 % larger than
498 ~~ecoregional late season fires, while early season fires grew 77 % larger than~~ late season fires ~~across the~~
499 ~~whole study region (Fig. 5). The relative increase~~largest difference in fire size ~~from~~between early
500 ~~season~~ignited and late ignited fires ~~compared to late season fires was more pronounced in~~was observed in
501 ~~the~~ southern ecoregions ~~than in northern ecoregions~~ (Table S9). ~~Alaska Boreal Interior, Taiga Plain, and~~

502 ~~Western Taiga Shield experienced the largest early season fires (23 218 (standard deviation: 7 557) ha)~~
503 ~~compared to the other ecoregions (9 922 (standard deviation: 5 192) ha)). However~~S10. Also, in these
504 ecoregions, ~~early season fires accounted for approximately one third of the total burned area whereas in~~
505 ~~the southern ecoregions~~ early-season fires accounted for more than half of the total burned area (Fig. ~~5 J,~~
506 ~~L, O and Table S9).~~5 J, L, O and Table S10) whereas in the northern ecoregions early-season fires
507 accounted for approximately one third of the total burned area. Across our study domain, the 20th
508 percentile earliest ignited fires accounted for an average of 40.6 (standard deviation: 14.2) % of the total
509 annual burned area (Table ~~S9).~~S10). Nonetheless, the largest early ignited fires on average were observed
510 in the forested ecoregions of Alaska Boreal Interior (Fig. 5A), Taiga Plain (Fig. 5E), and Western Taiga
511 Shield (Fig. 5G) (23 218 (standard deviation: 7 557) ha) compared to the other ecoregions (9 922
512 (standard deviation: 5 192) ha)).

513

514 3.5 Influence of ~~snowmelt~~snow disappearance timing on ignition timing

515 The pSEM for all ecoregions matched reasonably well with our hypothesized pSEM model (Fisher's C_{80}
516 = 82.24, $p = 0.41$; Fig. 6) and explained 38 % of the variation in the ~~snowmelt~~snow disappearance timing
517 (marginal R^2 (M- R^2) = 0.38, conditional R^2 (C- R^2) = 0.50) and 48 % of the variation in ignition timing
518 (~~fire weather:~~ M- $R^2 = 0.3514$, C- $R^2 = 0.3514$, and weather: M- $R^2 = 0.34$, C- $R^2 = 0.36$) (Fig. 6). The
519 model fits for ecoregions with earlier ~~snowmelt~~snow disappearance timing trend (Fisher's $C_{86} = 96.31$, p
520 = 0.21) and later ~~snowmelt~~snow disappearance timing trends (Fisher's $C_{112} = 107.14$, $p = 0.61$) ~~were~~
521 ~~poorer than~~showed similar patterns as the pSEM fit ~~on~~for all ecoregions (Fig. ~~S7).~~S8).
522 The variance explained in the ~~snowmelt~~snow disappearance timing and ignition timing were generally
523 better when splitting ecoregions between those with earlier ~~snowmelt~~and later snow disappearance trends
524 (~~snowmelt:~~ The pSEM model for earlier snow disappearance trends explained 32 % of the variation (M-
525 $R^2 = 0.32$, C- $R^2 = 0.32$,) while 54 % of the variation in ignition timing was explained by the model (fire
526 weather: M- $R^2 = 0.5415$, C- $R^2 = 0.54$) ~~and later snowmelt trends (snowmelt~~15, weather: M- $R^2 = 0.5339$,

527 C-R² = 0.53, ~~ignition: 39~~). The pSEM model for ecoregions with later snow disappearance trends
528 explained 53 % of the variation in the snow disappearance timing (M-R² = 0.53, C-R² = 0.5553) and 53 %
529 of the variation in ignition timing (fire weather: M-R² = 0.18, C-R² = 0.18, weather: M-R² = 0.35, C-R² =
530 0.37) (Fig. S7S8).

531 These results show that ~~snowmelt~~snow disappearance timing was driven by air temperature,
532 without significant influence of precipitation type and amount and humidity. The earlier ~~snowmelt~~snow
533 disappearance timing was correlated with high anomalies in air temperature, while the air temperature
534 was generally lower than the climatological averages with later ~~snowmelt~~snow disappearance timing
535 (Tables S10-S12S11-S13). The pSEM model results also show that earlier ~~snowmelt~~snow disappearance
536 timing promoted fuel drying across ecoregions (Fig. 6 and Table S10)-S11). This was also evident from
537 our alternative model which used ~~when using~~ vapor pressure deficit ~~rather than~~ instead of relative
538 humidity and air temperature (Fig. S9 and Tables. S14-S16)

539 ~~Snowmelt~~Snow disappearance timing itself had the strongest individual influence on ignition
540 timing across all ecoregions and models also after accounting for weather and fire weather. The cascading
541 effect of accelerated drying of organic soils from earlier ~~snowmelt~~snow disappearance timing carried over
542 to the timing of ignition. For all models, the DMC had the strongest influence on the ignition timing,
543 while the FFMC significantly affected ignition timing across all ecoregions and over the ecoregions
544 exhibiting earlier ~~snowmelt~~snow disappearance timing (Fig. 6, and Fig. S7aS8a). For ecoregions with
545 later ~~snowmelt~~snow disappearance trends, only the slow responding fuel moisture codes (DMC and DC)
546 significantly influenced the timing of ignition. For ecoregions with earlier ~~snowmelt~~snow disappearance
547 timing, DC influenced the ignition timing positively ~~and meaning that~~ earlier ignitions generally occurred
548 ~~under wetter when~~ DC ~~conditions was still low~~. The fuel moisture codes together ~~more strongly~~ influenced
549 the ignition timing ~~more strongly~~ compared to ~~snowmelt~~snow disappearance timing and weather variables
550 across models (Tables S10-S12S11-S13).

551 Early snowmeltsnow disappearance may also affect larger-scale atmospheric dynamics. We
552 found that earlier snowmeltsnow disappearance timing contributed to the destabilization of the
553 atmosphere through increased convective available potential energy (CAPE) across ecoregions (Fig. 6), in
554 particular for ecoregions with earlier snowmeltsnow disappearance timing (Fig. S7aS8a). Early
555 snowmeltsnow disappearance was associated with higher air temperatures and lower humidity in the
556 overall model. These favorable weather conditions led to earlier ignition in the overall model and the
557 model for ecoregions with earlier snowmeltsnow disappearance timing. Early ignitions were associated
558 with lower relative humidity and higher air temperatures driven by the earlier snowmeltsnow
559 disappearance timing (Fig. 6 and Fig. S7aS8a). Snow disappearance timing itself had the
560 strongest individual influence on ignition timing across all ecoregions and models. Similar results were
561 obtained when air temperature and relative humidity were as substituted by vapor pressure deficit (Fig. S9
562 and Tables S14-S16).

563

564 4. Discussion

565 4.1 Diverging spatial trends in snowmeltsnow disappearance timing and ignitions

566 We found the co-occurrence of a pronounced continental dipole in decadal trends of snowmeltsnow
567 disappearance timing and number of fire ignitions across arctic-boreal North America. We observed
568 increasingly earlier snowmeltsnow disappearance and an increase in the number of fire ignitions in
569 northwestern boreal North America between 1980 and 2019. In contrast, snowmeltsnow disappearance
570 timing has simultaneously been occurring later and the number of fire ignition decreased in the last
571 decades in the southeastern part of our study domain. The changes in snowmeltThe divergent trend in
572 number of ignitions is in accordance with a previous study on changes in the number of fires and burned
573 area across Canada from 1959 to 2015 (Hanes et al., 2019). The changes in snow disappearance timing
574 that we found in our study are corroborated by earlier work demonstrating both increasing and decreasing

575 trends in snow-cover over southeastern and northwestern boreal North America, respectively (Chen et al.,
576 2016). Furthermore, Bormann et al. (2018) found an earlier onset of spring snowmeltsnow disappearance
577 in northwestern boreal North America in contrast to later snowmeltsnow disappearance or no changes in
578 snowmeltsnow disappearance timing over southeastern boreal North America.

579 -We also found that the west-east diverging trend in snowmeltsnow disappearance timing has
580 become more pronounced in the last two decades compared to the longer-term trend since 1980. These
581 observations followed the divergent trend of less pronounced changes in long-term early spring air
582 temperature (1980-2019) and distinct dipoles in early spring air temperature over boreal North America
583 between 2001 and 2019 (Fig. S8S109). Similar to Cohen et al. (2014), we found small changes in air
584 temperature between 1980 and 2019 in the northern and southern parts of our study domain (Fig.
585 S8aS109a). The last two decades of enhanced west-east divergence in snowmeltsnow disappearance
586 timing followed the development of a pronounced west-east dipole in early spring air temperature as
587 observed in our linear-mixed effect models (Table S4S5) and also observed in two consecutive recent
588 winters between 2013 and 2015 (Singh et al., 2016). As higher early spring air temperatures promote
589 earlier snowmeltsnow disappearance, the snow-albedo feedback will in turn result in higher air
590 temperatures (Déry and Brown, 2007). In this way, the presence of a dipole of changes in early spring air
591 temperature and snowmeltsnow disappearance timing over boreal North America might indicate that both
592 processes re-enforce each other on sub-continental scales.

593 Besides regional changes in early spring air temperature, large-scale atmospheric dynamics may
594 also have influenced snowmeltsnow disappearance timing and the number of ignitions as observed in our
595 study (Cohen et al., 2014; Zhao et al., 2022). Changes in sea ice and snow cover (Zou et al., 2021) may
596 have large impact on the location of the polar jet stream and tropospheric ridge persistency causing air
597 temperature extremes (Francis and Vavrus, 2012; Kim et al., 2014; Horton et al., 2016). In recent
598 decades, these persistent tropospheric ridge patterns have been located over the northwestern part of our
599 study domain which traps and slows the progression of Rossby waves eastwards (Francis and Vavrus,

600 2012; Jain and Flannigan, 2021) resulting in downstream troughing over the east (Singh et al., 2016). This
601 tropospheric ridge leads to a blocked anticyclone in the west, causing higher air temperatures and
602 increased burned area, and an associated cyclone over eastern North America with lower air temperatures
603 and less burned area (Skinner et al., 1999; Cohen et al., 2014; Sharma et al., 2022). Further, the
604 stratospheric vortex, westerly winds formed in the stratosphere during winter time, may have weakened
605 and consequently sudden stratospheric warming (SSW), rapid heating in the stratosphere over the North
606 Pole, have caused winter cold-spells over eastern Canada over the last four decades (Kretschmer et al.,
607 2018b). The effect of winter cold-spells may carry over into spring delaying the snowmeltsnow
608 disappearance timing and thus the fire season.

609 -The presence of a dipole in snowmeltsnow disappearance timing and ignition trends in our study
610 is likely related to: (1) changes in the stratospheric vortex and SSW that send winter cold-spells over the
611 eastern part of the study domain (Kretschmer et al., 2018a) and as a consequence annual mean air
612 temperature anomalies divergence from increasing in the west to decreasing in the east of boreal North
613 America in the last decades (Cohen et al., 2012; Coumou et al., 2018). (2) Changes in the location of the
614 summer jet as a consequence of longer persistence of positive geopotential anomalies over the western
615 part of our study domain (Jain and Flannigan, 2021; Zou et al., 2021). ~~However~~Although our results do
616 not provide clear indications, the persistent ridge formation could possibly also be a result of the
617 divergent snowmeltsnow disappearance trend caused by the SSW. Both the soil moisture and albedo
618 feedback between snowmeltsnow disappearance timing and air temperature may have further
619 ~~strengthened~~ strengthening the diverging trends. ~~These processes may also have triggered and influenced~~
620 the persistency of the severe fire season fire extremes across Canada in 2023. In our study, Our results
621 suggest that these atmospheric processes and soil moisture feedbacks may also have led to the enhanced
622 fuel dryness in western ecoregions that has driven the large increases in number of ignitions compared to
623 the other ecoregions (Abatzoglou and Williams, 2016; Holden et al., 2018).

624

625 4.2 Influence of snowmeltsnow disappearance timing on ignition timing and fire size

626 By focusing on the start of the fire season, we were able to disentangle the effect of snowmeltsnow
627 disappearance timing on ignition timing. Previous studies found no significant effects of snowmeltsnow
628 disappearance timing on annual burned area, with snowmeltsnow disappearance timing being regarded as
629 a minor driver of annual burned area compared to meteorological variables (Jolly et al., 2015; Kitzberger
630 et al., 2017). Nonetheless, snowmeltsnow disappearance timing has shown to play a crucial role in
631 altering fuel dryness and the frequency of large fires over a temperate forest in the western United States
632 (McCammon, 1976; Westerling et al., 2006). Our results show that snowmeltsnow disappearance timing
633 has a strong influence on early ignition timing and fire size~~early fire characteristics~~ in all ecoregions of
634 boreal North America. This relationship diminished when snowmeltsnow disappearance timing was
635 compared to progressively later ignitions (Fig. S3S4). This may be due to the importance of the spring
636 window, the period between snowmeltsnow disappearance timing and leaf flush, on early-season fires
637 (Parisien et al., 2023). During the spring window deciduous and mixed forests are very conducive to fire
638 and ecoregions experience the longest spring window corresponded to where we also found the highest
639 early fire ignition density (Fig. 5J, L-M) (Parisien et al., 2023). Also, the longest spring window was
640 found in the interior west of Canada (Parisien et al., 2023), which coincides with the ecoregions with most
641 fire ignitions observed in our study (Fig. 1). Late-season ignitions in July, August and September may be
642 more influenced by long-term drought and synoptic weather conditions than by snowmeltsnow
643 disappearance timing (Jain et al., 2017; Holden et al., 2018).

644 We fouind that throughout boreal North America, fires caused by early season ignitions following
645 earlier snowmeltsnow disappearance also on average grew larger than fires ignited in the late fire season.
646 This was in accordance with earlier findings limited to Alaska, USA, and the Canadian Northwest
647 Territories (Veraverbeke et al., 2017). Because of the early snowmeltsnow disappearance and the earlier
648 ignition timing, early season fires have longer temporal windows with potential for favorable warm and
649 dry weather conditions conducive to fire spread (Sedano and Randerson, 2014). Indeed, the 20 % earliest

650 ignitions resulted in approximately 40 % of the total burned area across the study domain between 2001
651 and 2019. In the future, the contribution of early fires to burned area might increase with warmer and
652 drier weather conditions leading to earlier ~~snowmelt~~snow disappearance and thus an increased likelihood
653 for earlier and larger fires over boreal North America (Flannigan et al., 2005, 2013).

654

655 *4.3 Changes in the snow-free and fire season lengths*

656 We found a north-south gradient in the changes in the actual fire season length ranging from a prolonging
657 of 30 days per decade in northern ecoregions to a shortening of 25 days per decade in southern
658 ecoregions. Previous studies have mainly found the prolonging of the potential fire season to be between
659 3 and 30 days per decade over boreal North America (Wotton and Flannigan, 1993; Flannigan et al.,
660 2013; Jolly et al., 2015; Jain et al., 2017). These estimates of the prolonging of the potential fire season
661 were based on changes in fire weather (Flannigan et al., 2013; Jain et al., 2017). Other studies ~~have,~~
662 ~~with that examined the usage of~~ governmental fire perimeter data, also found a prolonging of the fire
663 season length limited to the western North America, ~~Alberta and Ontario in Canada (Westerling et al.,~~
664 ~~2006; Albert Green et al., 2013); (Westerling et al., 2006; Albert-Green et al., 2013; Hanes et al., 2019).~~ In
665 our study, we used daily fire spread data derived from ~~spaceborne data~~satellite observations to determine
666 the fire season start and end dates (Skakun et al., 2021; Potter et al., 2023). This approach, however, relies
667 on MODIS active fire data and therefore is limited to the MODIS era in the 2000s. Longer-term accurate
668 temporal and spatial data on ignition timing and end of burning is needed to assess the changes in the
669 actual fire season on a climatic timescale and a continental scale. Our results suggest that a change in the
670 duration of the snow-free season is almost one to one related to a change in the duration of the fire season
671 across boreal and ~~arctic~~Arctic North America. However, the effect may be of more importance on the fire
672 season start than the end of the fire season as this is often marked by the first rainfall in autumn in
673 adequate amounts for extinguishing fires and rewetting dried out fuels preventing new ignitions. Climate
674 change induced changes in the amount and timing of autumn rainfall will likely effect the timing of the

675 fire season end (Holden et al., 2018; Goss et al., 2020). Although, recent studies also showed that some
676 fires overwinter and re-emerge the following spring (McCarty et al., 2020; Scholten et al., 2021b; Xu et
677 al., 2022), challenging the concept of a demarcated fire season. In a warmer North American Arctic-
678 boreal region, the snow-free season will likely prolong with a consequent lengthening of the fire season,
679 both starting earlier in spring and prolonging later into autumn (Flannigan et al., 2013).

680

681 4.4 Cascading effects of snowmeltsnow disappearance timing on weather and ignition timing

682 In the three piecewise structural equation models (pSEMs), anomalies in snowmeltsnow disappearance
683 timing were only attributed to anomalies in air temperature (hypothesis 1). Our models did not confirm
684 the importance of the amount or the type of precipitation for snowmeltsnow disappearance timing
685 observed in previous research (hypothesis 2) (Barnett et al., 2005; McCabe et al., 2007). However, air
686 temperature also affected precipitation types in our models which, although statistically insignificant,
687 showed divergent influences on snowmeltsnow disappearance timing between ecoregions with earlier and
688 later snowmeltsnow disappearance trends (Tables S11S12 and S12S13). This suggests that the air
689 temperature dipole observed in the last two decades (Fig. S8S109) may influence precipitation, including
690 snowpack volume and persistency (Brown and Mote, 2009) and therefore likely also snowmeltsnow
691 disappearance timing (Barnett et al., 2005). Nonetheless, snowmeltsnow disappearance timing itself
692 largely influenced ignition timing regardless of ignition source and ecoregion, and we additionally found
693 snowmeltsnow disappearance timing to be an important early indicator for early season fires in the North
694 American Arctic-boreal region (hypothesis 3). ~~We~~Our model also ~~found~~suggests a cascading effect of
695 snowmeltsnow disappearance timing on meteorological conditions that carried over into the influence on
696 ignition timing. Relationships between warm and dry conditions and ignitions and fire spread have been
697 established before (Sedano and Randerson, 2014; Veraverbeke et al., 2017). This was only apparent for
698 the overall model and the model including ecoregions with earlier snowmeltsnow disappearance timing
699 (hypothesis 4). This suggests that land-atmosphere dynamics are altered by changes in snowmeltsnow

700 disappearance timing as it influences the soil moisture content which is proportional to evapotranspiration
701 changing the land energy balance (Seneviratne et al., 2010). Also, this in combination with anomalously
702 high springtime air temperatures promoted greening of vegetation and desiccation of soils in other boreal
703 regions changing the impact of the warming in the atmospheric (Gloege et al., 2022). These land-
704 atmosphere dynamics may have been potential pathways for extreme fire seasons in Siberia (Scholten et
705 al., 2022), and our pSEM results indicatesuggest that similar dynamics may be in place over ecoregions
706 with earlier snowmeltsnow disappearance timing. The ecoregions with later snowmeltsnow disappearance
707 timing, which ~~did not show this~~showed less carry-over effect of snowmeltsnow disappearance timing on
708 weather and fuel moisture to ignition, also corresponded to the more densely populated regions. ~~This may~~
709 ~~be due to the elevated potential for anthropogenic ignitions that again coincide with the more flammable~~
710 ~~vegetation during the spring window~~ with larger fraction of deciduous trees (Pavlic et al., 2007; Olthof et
711 al., 2015). The lack of carry-over effect may be due other drivers such as elevated potential for
712 anthropogenic ignitions and the spring window during which deciduous forests are most flammable
713 (Wotton et al., 2010; Parisien et al., 2023) ~~and less with favorable weather conditions compared to~~
714 ~~lightning ignitions.~~

715 The results of our study also point to cascading effects of changes in snowmeltsnow
716 disappearance timing on dry fuel availability that carried over into the ignition timing across all models.
717 The fine fuel moisture and duff moisture codes showed significant influences on ignition timing, while
718 the drought code did not, possibly due to its slower response to changes in weather (hypothesis 5). This is
719 in agreement with previous studies that indicate that the ignition of fires in boreal North America strongly
720 depends on the immediate dryness of the fine fuels (Abatzoglou and Williams, 2016; Hessilt et al., 2022).
721 The effects of earlier snowmeltsnow disappearance timing on enhanced desiccation of fuels observed in
722 three forests sites (McCammon, 1976) may be broadly applicable across boreal North America. As
723 observed in our study, dry fuels can directly promote ignition timing as they are readily ignitable (Hessilt
724 et al., 2022), but this may also be indirect through the influence on aboveground biomass senescence and

725 ecosystem production (Liu et al., 2020). Lastly, the changes in fuel moisture as a consequence of snow
726 disappearance can also play a role in the soil moisture-climate interaction which is not accounted for in
727 this model.

728 ~~Our pSEM analysis gives a simplified overview of relationships between snowmelt~~
729 ~~disappearance timing, land-atmosphere dynamics, and fire ignitions. However, we acknowledge that these~~
730 ~~interactions are highly coupled. The influence of snowmelt~~~~disappearance timing on atmospheric~~
731 ~~variables through surface albedo change and altered soil moisture may be difficult to decouple from the~~
732 ~~atmospheric variables and their persistent seasonal patterns on snowmelt~~~~disappearance timing itself.~~
733 ~~We therefore call for a better understanding of the role of snowmelt~~~~disappearance timing on land-~~
734 ~~atmospheric dynamics affecting boreal fires. Specifically, large-scale influence of continuous~~
735 ~~snowmelt~~~~disappearance on soil and fuel properties, e.g. soil and fuel moisture, and atmospheric~~
736 ~~conditions e.g. vapor pressure deficit, and vice-versa. Understanding these interactions and feedbacks~~
737 ~~could further advance our comprehension of how climate change is affecting changing boreal fire~~
738 ~~regimes.~~

739

740 4.5 Limitations

741 We used a conservative threshold of 14 consecutive days of snow free pixels (NDSI \leq 15 %) to calculate
742 the snow disappearance timing. This could potentially influence the timing of snow disappearance to
743 occur later than observed. A comparison of snow disappearance timing retrieval with a threshold of seven
744 consecutive days of snow free pixels indicated that the retrievals resulted in similar temporal patterns in
745 snow disappearance timing regardless of threshold choice (Fig. S1, Table S2), with the 14-days threshold
746 generally resulting in later snow disappearance timing. The largest discrepancies between the retrievals of
747 snow disappearance timing with different temporal thresholds were found in the southern ecoregions
748 (Table S2). This indicates that the threshold of 14 consecutive days with snow free pixels may be more

749 robust to determine snow disappearance timing, because of sudden changes in weather can manifest in
750 snow offset and onset, especially in southern ecoregions.

751 The long-term and short-term trends of snow disappearance timing and number of ignition were
752 not consistently statistically significant for all ecoregions. The uncertainty related to the retrieval of both
753 snow disappearance timing and fire perimeters from the pre-MODIS era (before 2000) resulted in large
754 variation in both variables. More robust findings could potentially be drawn with longer time series. Also
755 continued monitoring of snow disappearance and ignition timing is needed to track the relationship
756 between these two variables as their relationship may become more pronounced with further climate
757 change. Similarly, longer and more consistent time series could increase the robustness of the analysis on
758 snow-free vs. fire season length. While we observed a significant relationship between these variables
759 across ecoregions (Fig. 4c), this was not evident for most ecoregions (snow-free periods: $p < 0.1$ in six
760 ecoregions and fire season length: $p < 0.1$ for two ecoregions). We only used the shorter time period
761 between 2001 and 2019 data to establish these changes as these represent the higher quality data during
762 the MODIS era.

763 Lastly, our pSEM analysis gives a simplified overview of relationships between snow
764 disappearance timing, land-atmosphere dynamics, and fire ignitions. However, we acknowledge that these
765 interactions are highly coupled. The complexity is beyond our model and may involve variables that we
766 did not include. The influence of snow disappearance timing on atmospheric variables through surface
767 albedo change and altered soil moisture may be difficult to decouple from the atmospheric variables and
768 their persistent seasonal patterns on snow disappearance timing itself. Our models provide further support
769 of the importance of land-atmosphere dynamics in relation to fire, yet our analysis did not provide robust
770 relationships explaining the mechanistic interactions. We therefore call for a better understanding of the
771 role of snow disappearance timing on land-atmospheric dynamics affecting boreal fires. Specifically,
772 large-scale influence of continuous snow disappearance on soil and fuel properties, e.g. soil and fuel
773 moisture, and atmospheric conditions e.g. vapor pressure deficit, and vice versa. Understanding these

774 interactions and feedbacks could further advance our comprehension of how climate change is affecting
775 changing boreal fire regimes. Lastly, we modelled complex land-atmosphere interactions, including
776 relationships between snow disappearance timing, weather and ignition timing, using simple pSEMs. The
777 interactions may be more complex and include other variables on different scales that we did not include
778 in our analysis. Our models provide further support of the importance of land-atmosphere dynamics in
779 relation to fire, yet our analysis did not provide robust relationships explaining the mechanistic
780 interactions. We therefore call for further investigation of the interactions between snow disappearance
781 timing, atmospheric conditions, and their influences on the fire season start, length, extent and severity.

782

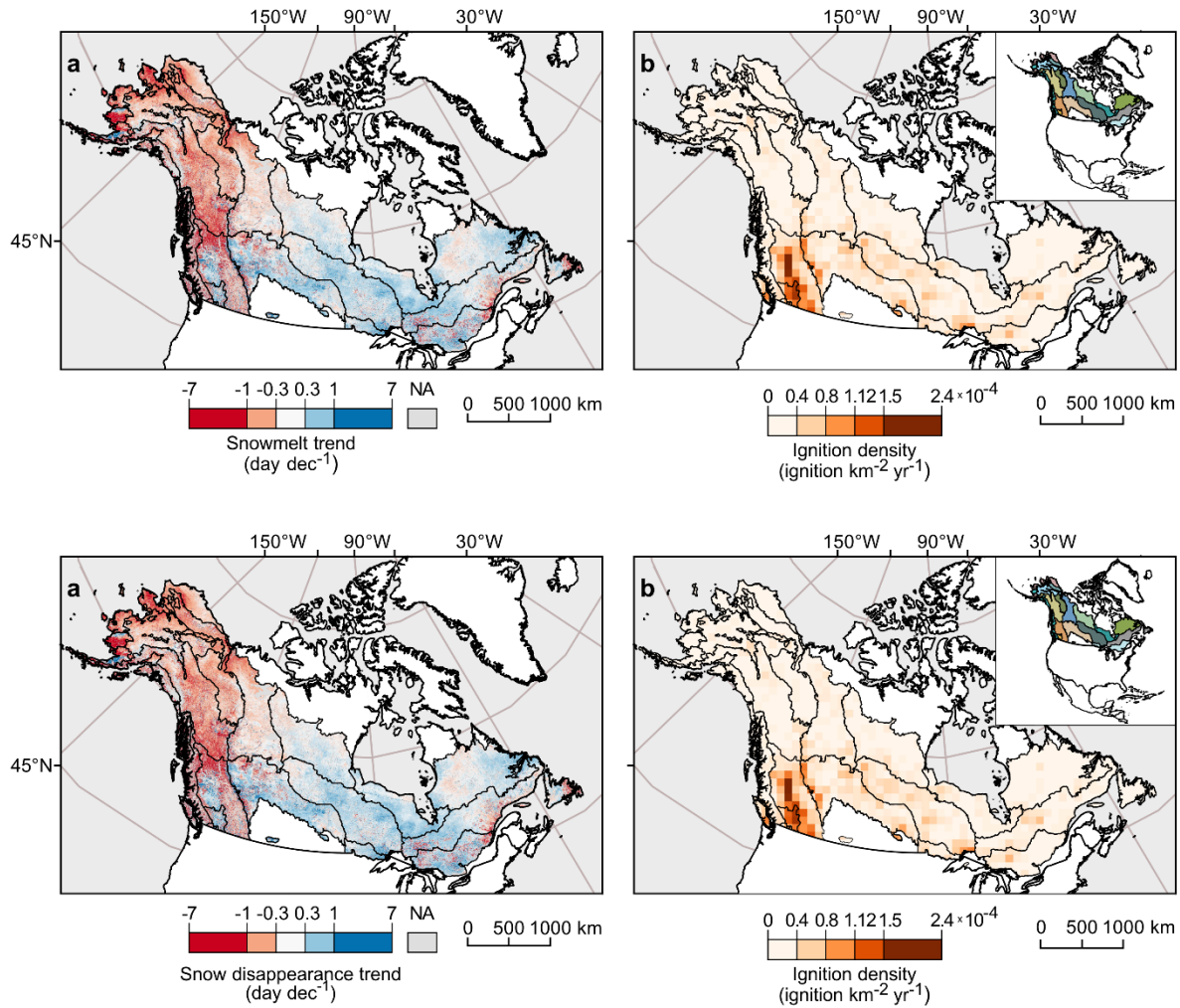
783 **5. Conclusions**

784 We found a pronounced west-east divergence of recent changes in snowmelt/snow disappearance timing
785 and the number of fire ignitions across boreal North America. Our results point to a clear trend of earlier
786 spring snowmelt/snow disappearance in the northwestern ecoregions, while the southern and eastern
787 ecoregions showed an increasingly later snowmelt/snow disappearance timing over the last decades.
788 Similarly, the total number of fire ignitions increased in the northern and western ecoregions, while the
789 southeastern ecoregions experienced little to no changes in the number of early fire ignitions. We
790 conclude that climate warming resulted in increasingly earlier snowmelt/snow disappearance in north-
791 western boreal North America, which in turn led to earlier fire ignitions, which tended to grow into larger
792 fires.

793 The temporal trends in snowmelt/snow disappearance and ignitions across boreal North America
794 followed the same spatial pattern of temporal trends in early spring air temperature over the last four
795 decades. Snowmelt/Snow disappearance and ignition timing were positively correlated across all
796 ecoregions and earlier snowmelt/snow disappearance was also the main driver for earlier fire ignitions
797 across all ecoregions. Further, we found a cascading effect of elevated air temperature and earlier

798 snowmeltsnow disappearance that carried over into earlier drying of fuels, which resulted in earlier
799 ignitions across the study domain. This cascade was more pronounced over ecoregions with increasingly
800 earlier snowmeltsnow disappearance timing than over those with increasingly later snowmeltsnow
801 disappearance timing. Our work points to the important impact that snow cover and snowmeltsnow
802 disappearance timing have on fire ignitions and fire size across boreal North America, as well as the
803 influence of changes in snowmeltsnow disappearance timing on changes in fire regimes. In a warming
804 North American boreal forest, earlier snowmeltsnow disappearance will likely result in increasingly
805 earlier and larger fires.

806



807

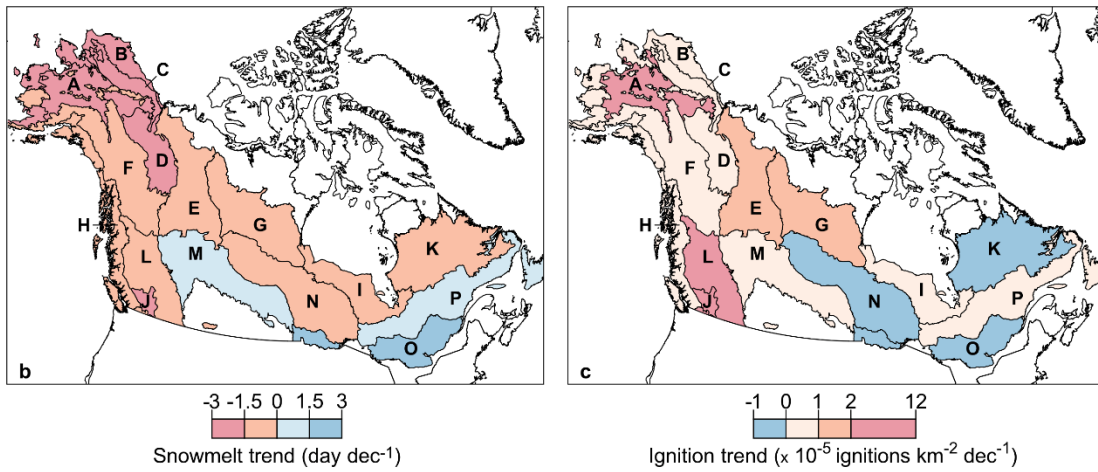
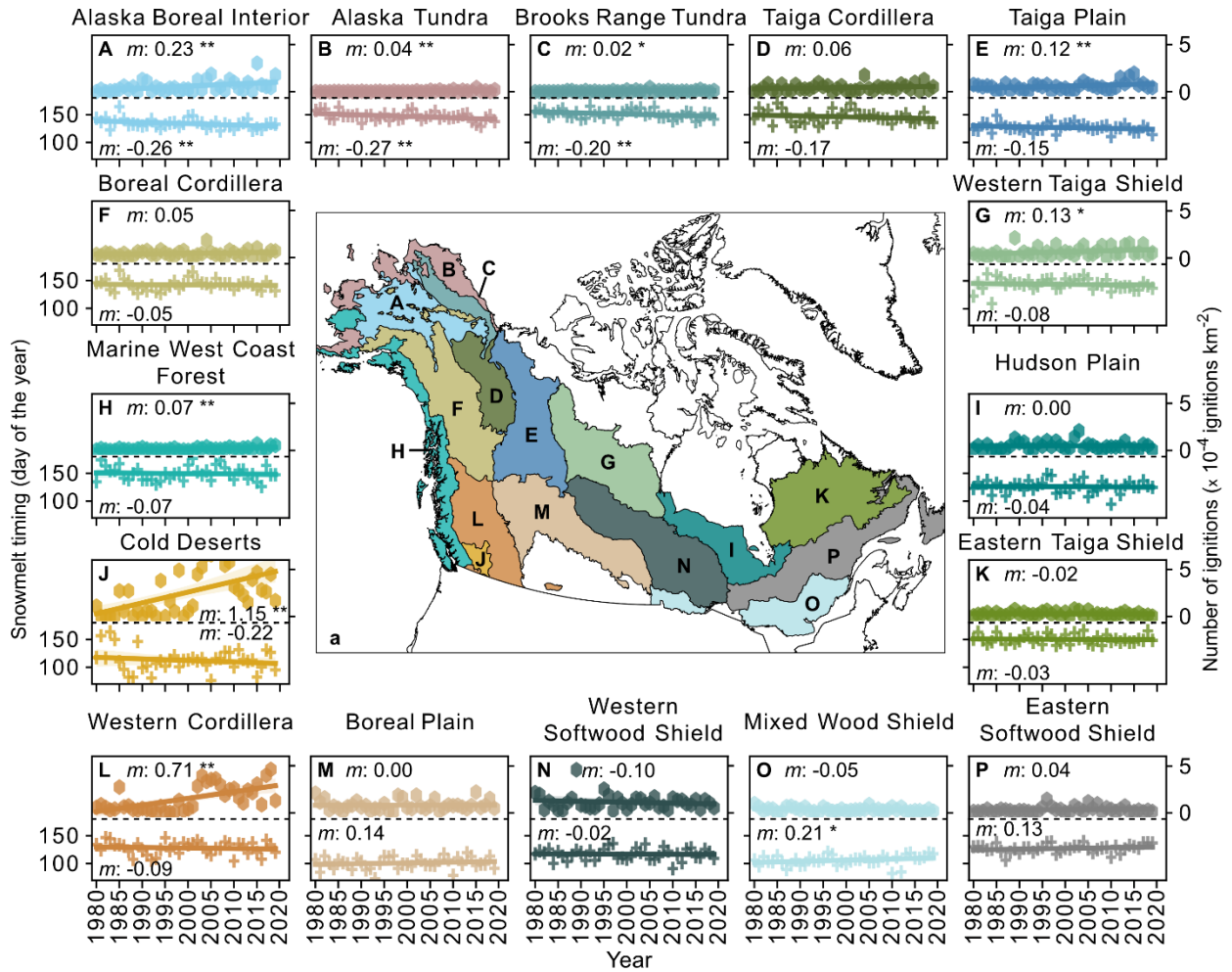
808

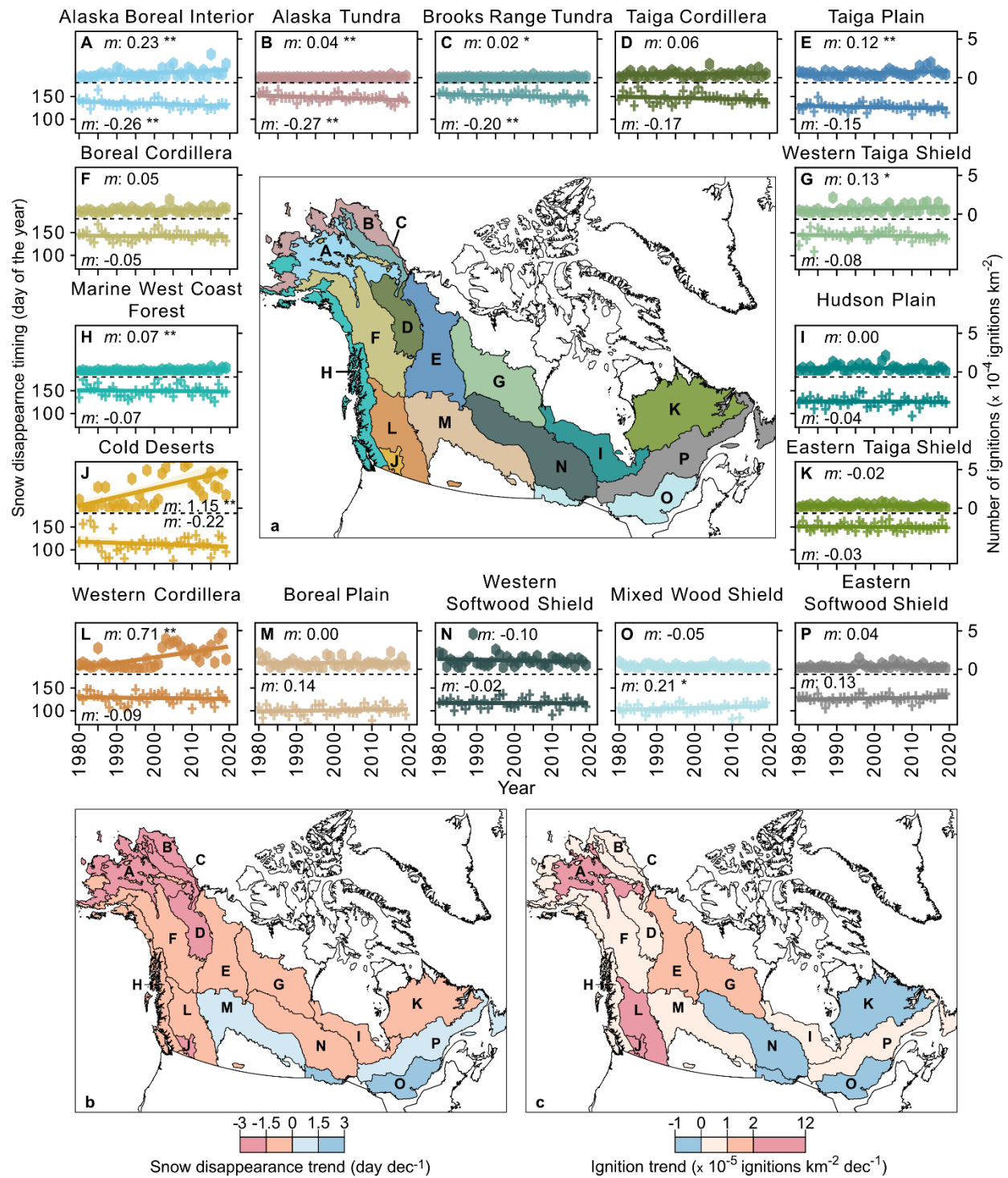
809

810

811

Figure 1 (a) Trend in snowmeltsnow disappearance timing between 2001 and 2019 derived from Moderate Resolution Imaging Spectroradiometer (MODIS) for the study domain overlaid by second-level ecoregions (US EPA, 2015) and (b) the mean annual ignition density per 100 x 100 km grid cells between 2001 and 2019. All pixels exceeding the average pixel snowmeltsnow disappearance timing ± 3 standard deviation were excluded and set to not applicable (NA: grey).



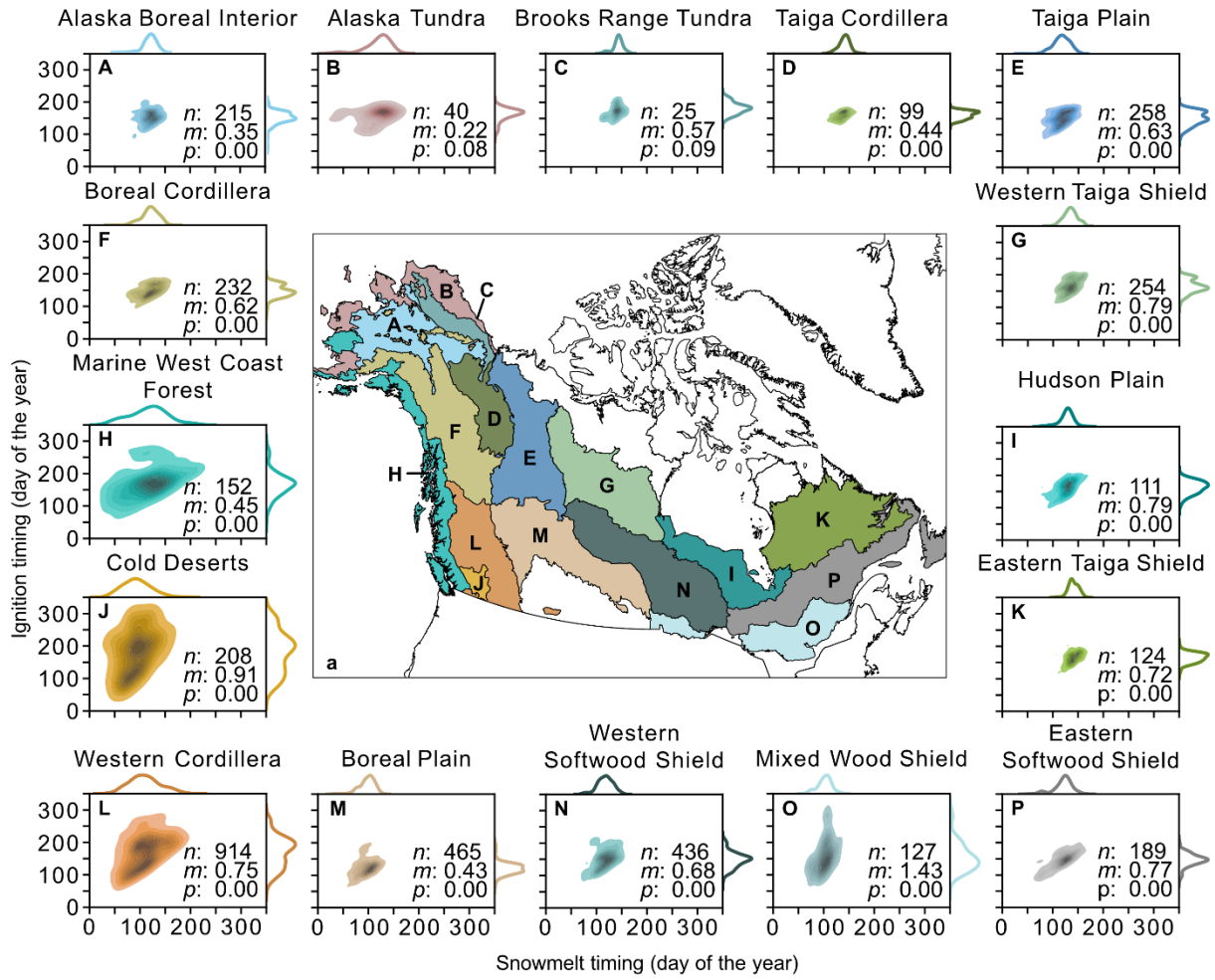


813

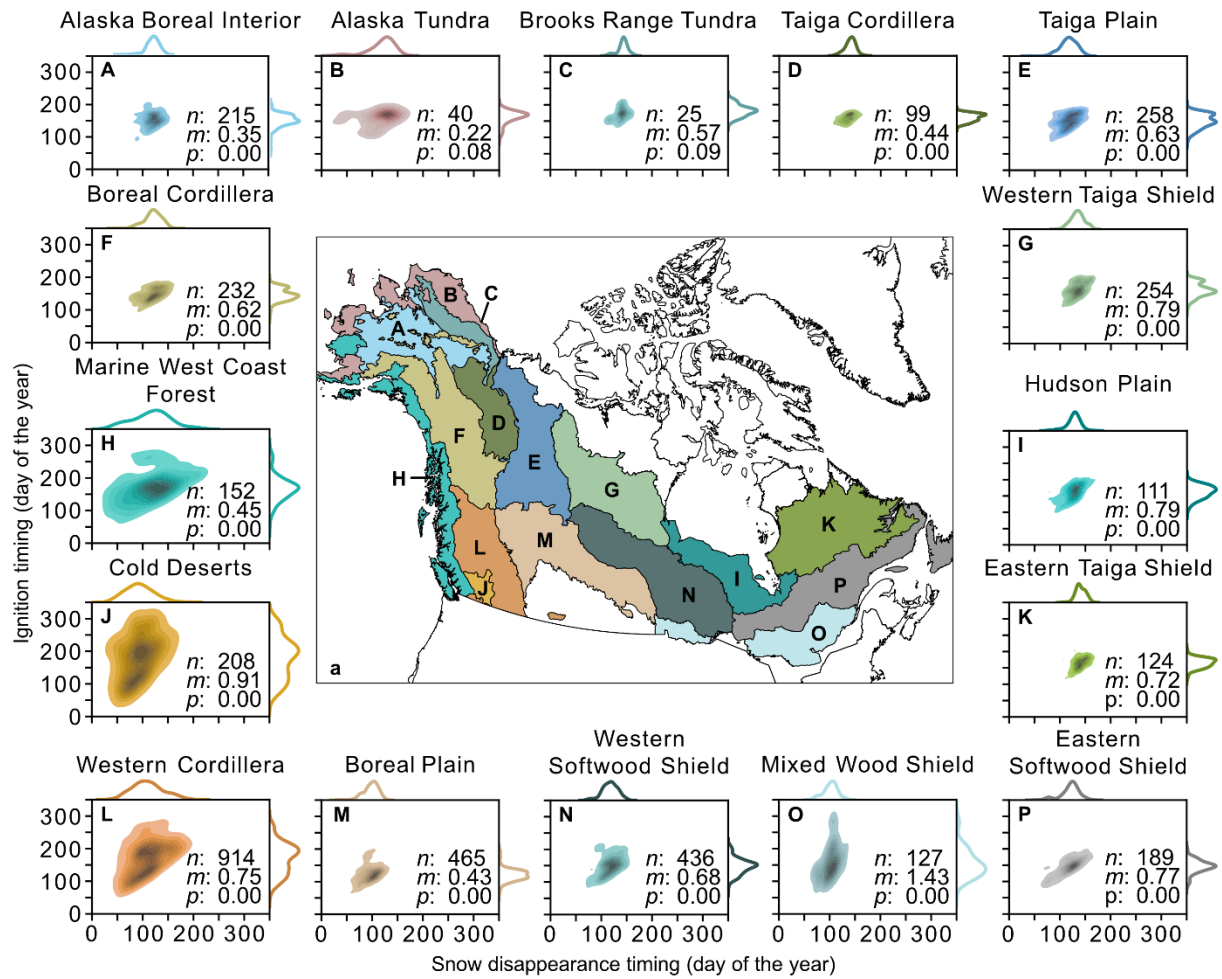
814 **Figure 2** Trends in ~~snowmelt~~ snow disappearance timing and ignitions for all ecoregions (A-P) between 1980 and 2019 (a). The

815 slope is given for all ecoregions, and its significance level is indicated by * ($p < 0.1$) or ** ($p < 0.05$). The magnitude and

816 direction of the long-term trends in daily ~~snowmelt~~ snow disappearance timing (b) and number of ignitions (c) from 1980 to 2019.

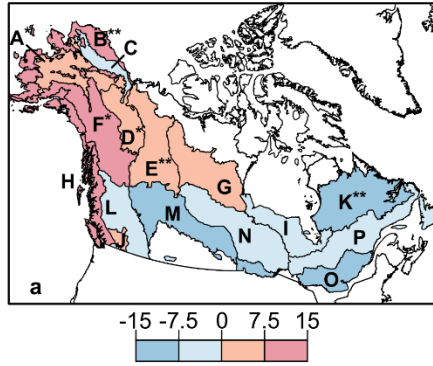


817

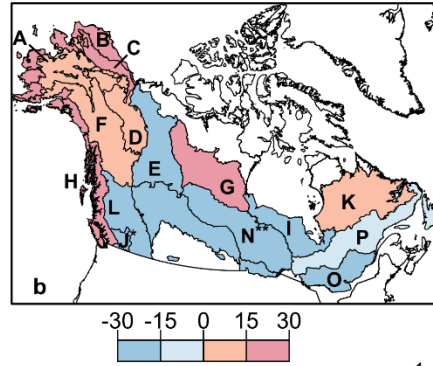


818

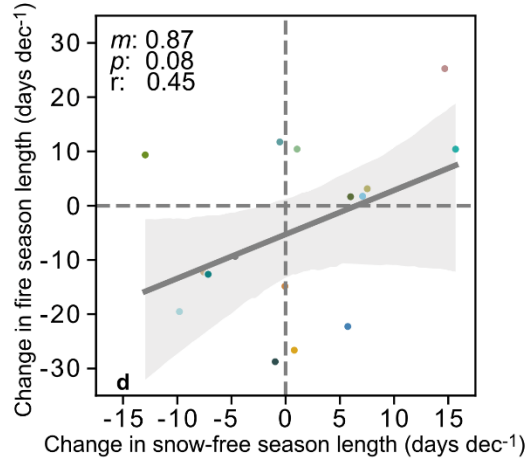
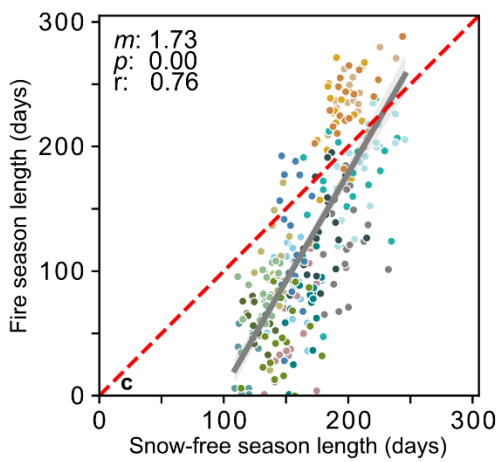
819 **Figure 3** Relationship between snowmelt/snow disappearance and ignition timing for all ignitions of the annual 20th percentile of
 820 the ignitions timing distribution per ecoregion, and their density plots (A-P). The number of ignitions (*n*), the slope (*m*), and the
 821 significance level (*p*) are indicated for each ecoregion.



Change in snow-free season length (days dec⁻¹)



Change in fire season length (days dec⁻¹)



- | | | | |
|--------------------------|----------------------------|---------------------------|------------------------|
| ● Alaska Boreal Interior | ● Brooks Range Tundra | ● Mixed Wood Shield | ● Taiga Plain |
| ● Alaska Tundra | ● Cold Deserts | ● Eastern Softwood Shield | ● Eastern Taiga Shield |
| ● Boreal Cordillera | ● Hudson Plain | ● Western Softwood Shield | ● Western Taiga Shield |
| ● Boreal Plain | ● Marine West Coast Forest | ● Taiga Cordillera | ● Western Cordillera |

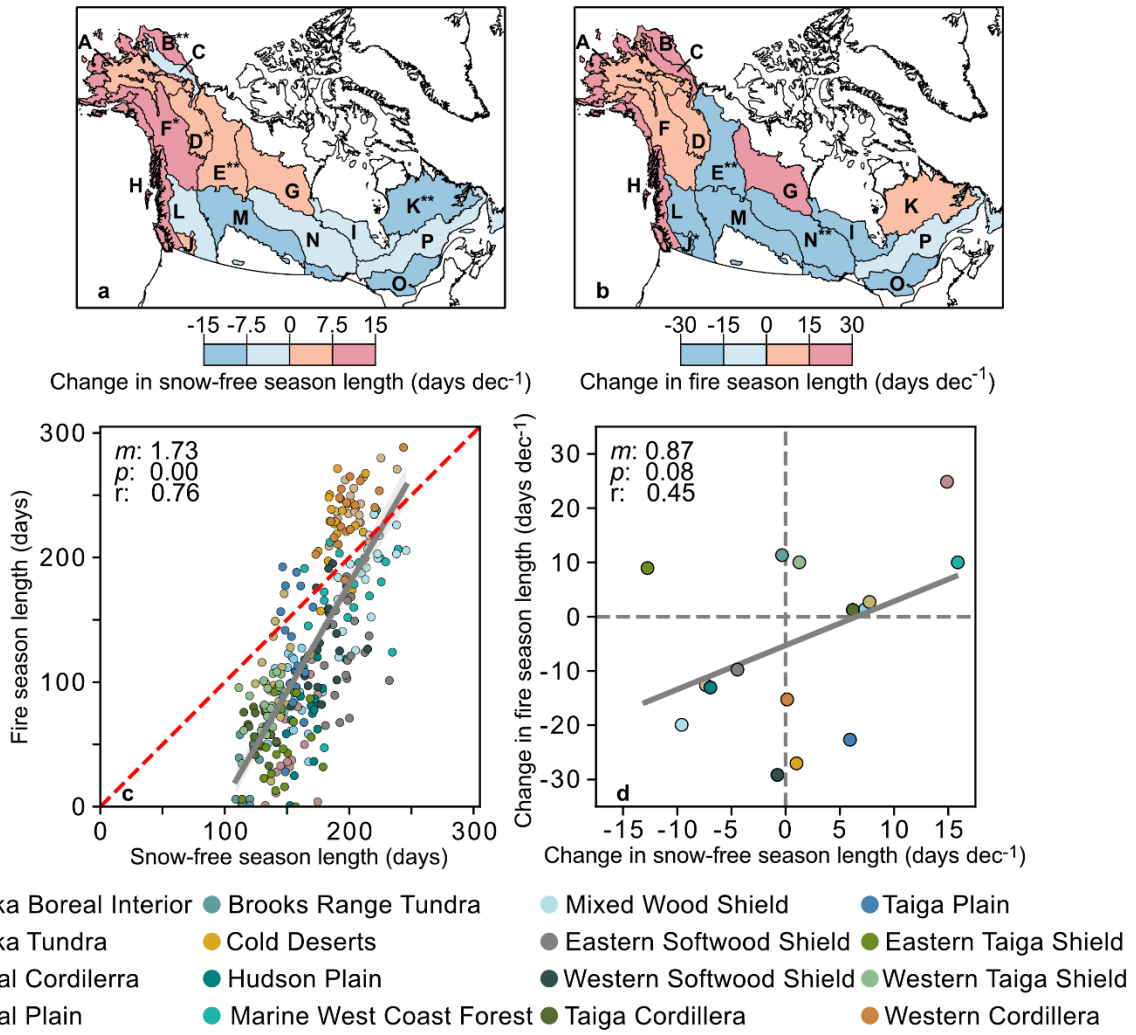
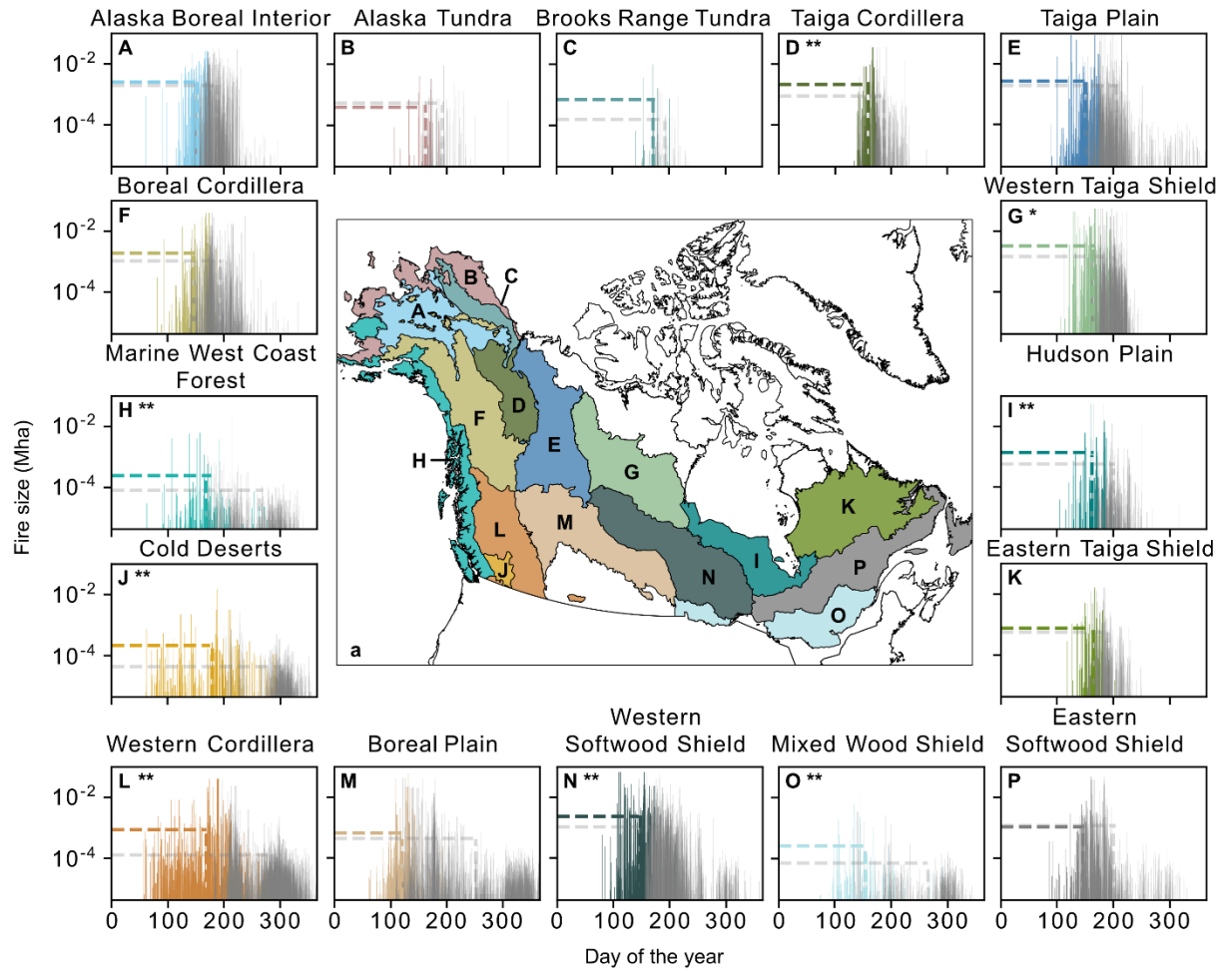
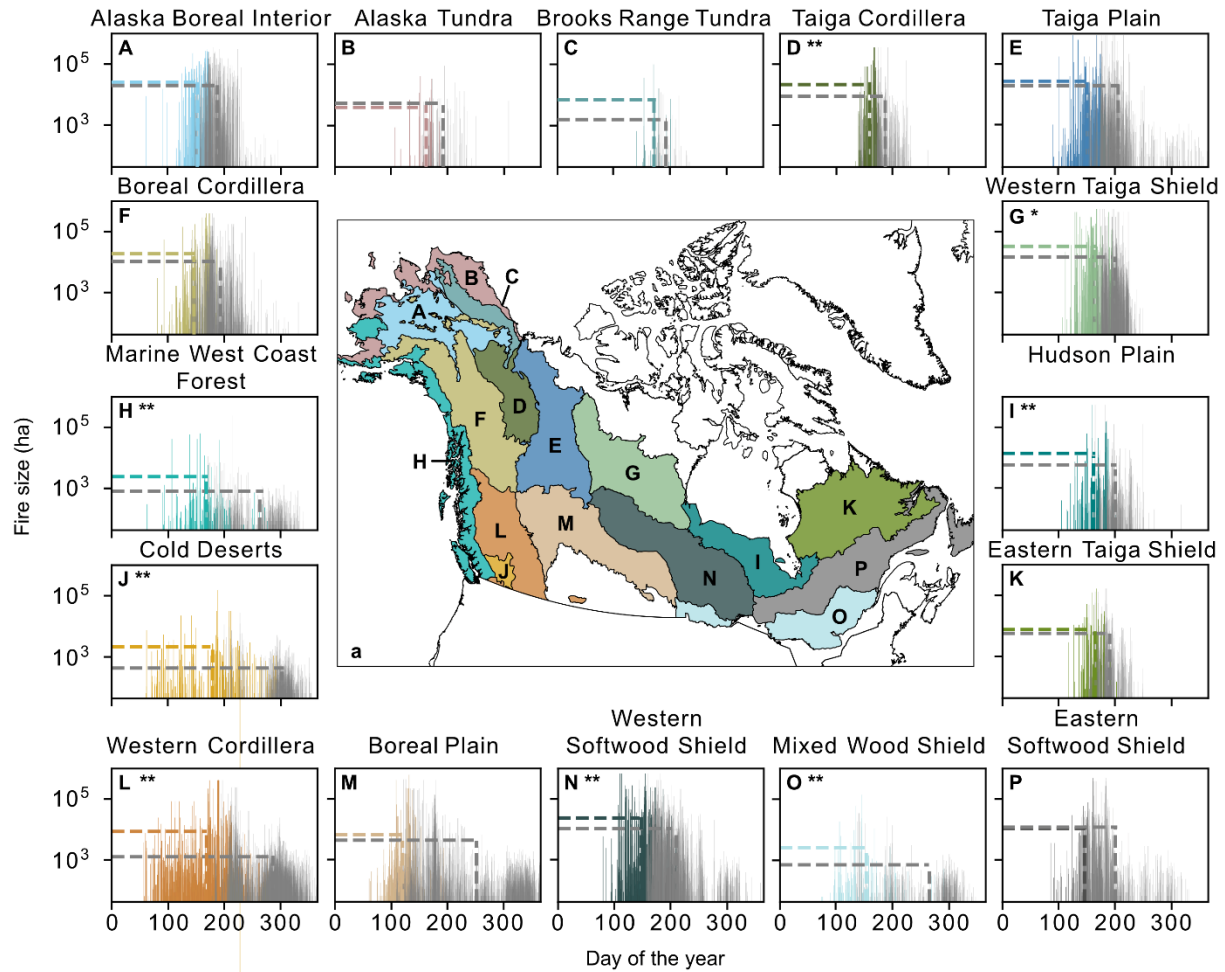


Figure 4 Changes the snow-free season length (days decade⁻¹) for all ecoregions (A-P) between 2001 to 2019 (a), and the changes in the fire season length (days decade⁻¹) per ecoregion (A-P) between 2001 to 2019 (b) (Table [S9S10](#)). Letters correspond to the respective ecoregion names (Fig. 2) and significant relationships are indicated by * ($p < 0.1$) and ** ($p < 0.05$). The relationship between the annual absolute length of the snow-free season from the MODIS-product (days) and annual length of the fire season for all ecoregions (c), and the ecoregional trends in snow-free and fire season length (days dec⁻¹) (d).



830

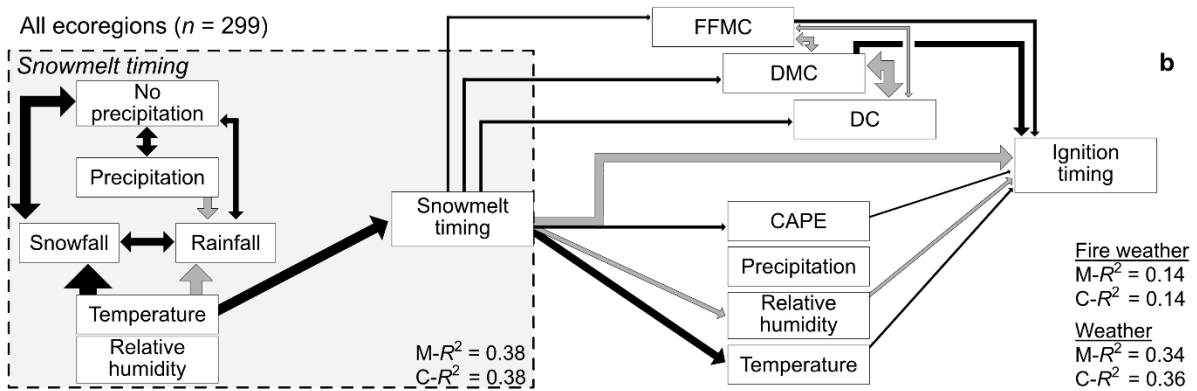
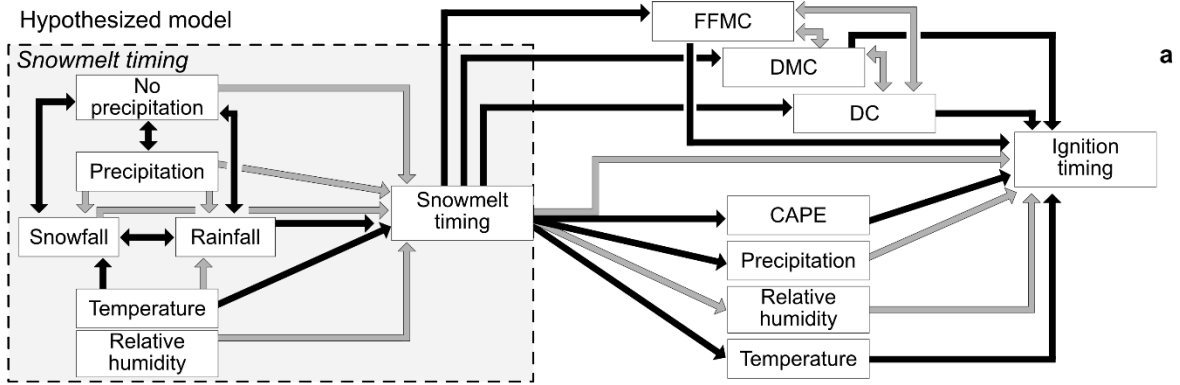


831

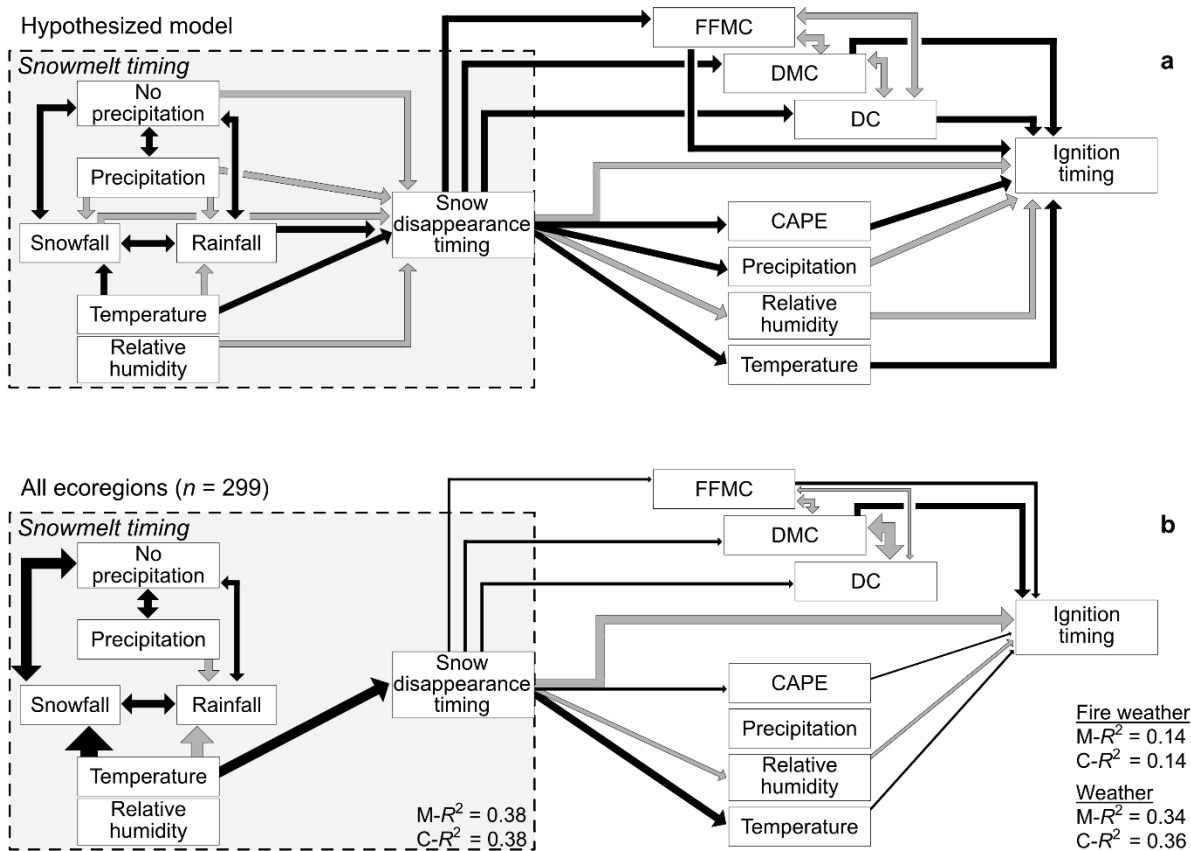
832 **Figure 5** Fire size as a function of ignition timing for all ecoregions (A-P). The 20th percentile day of ignition was set as
 833 threshold to discriminate between early (colored) and late season fires (gray). The colored dashed lines indicate the mean
 834 ignition timing and fire size for all early season ignitions while the gray dashed lines indicate the mean ignition timing and fire
 835 size for all late season ignitions. Significant larger difference between fire sizes of early season and late ignited fires were
 836 indicated by * ($p < 0.1$) and ** ($p < 0.05$). Note the logarithmic scale for fire size.

837

838



839



840

841 **Figure 6** Piecewise structural equation model (pSEM) of the hypothesized ~~snowmelt~~ snow disappearance and ignition timing
 842 model (a) and its fit for all ecoregions (b). The influence of fire weather and weather on ignition timing were modelled
 843 separately. Gray arrows represent positive effects and black arrows indicate negative effects. The single-headed arrows show
 844 significant direction of causal relationships, while double-headed arrows represent significant non-causal relationships ($p <$
 845 0.051). All arrows are scaled to their respective effect size (Table ~~S10S11~~). Marginal R² (M-R²) indicates the variation solely
 846 explained by the fixed effects and conditional R² (C-R²) represents the variation explained by both the fixed and random effects.

847

848 **Code availability**

849 Code is available upon request from the corresponding author.

850 **Data availability**

851 The [Moderate Resolution Imaging Spectroradiometer \(MODIS\)](#) and [National Snow and Ice Data Center](#)
852 [\(NSIDC\)](#) snow cover data is publicly available from the National Snow and Ice Data Center (MODIS:
853 <https://nsidc.org/data/mod10a1/versions/6>, NSIDC: <https://nsidc.org/data/nsidc-0046/versions/4>). The
854 burned area data is publicly available from the Oak Ridge National Laboratory Distributed Active
855 Archive Center for Biogeochemical Dynamics (ORNL-DAAC)
856 (<https://doi.org/10.3334/ORNLDAAAC/2063>). Fire ignition data from Alaska, Yukon, and the Northwest
857 Territories is available from the ORNL DAAC (<https://doi.org/10.3334/ORNLDAAAC/1812>). ~~The ignition~~
858 ~~data across boreal North America that we generated in this study is publicly available from the ORNL-~~
859 ~~DAAC (<https://doi.org/10.3334/ORNLDAAAC/2316>).The ignition data across boreal North America that~~
860 ~~we generated in this study is under the process to become freely available on the ORNL DAAC.~~ All
861 meteorological and fire weather variables were derived from the fifth generation of the European Centre
862 for Medium- Range Weather Forecast; (meteorological variables:;
863 <https://cds.climate.copernicus.eu/cdsapp#!/dataset/reanalysis-era5-single-levels?tab=overview>, and fire
864 weather indices: <https://cds.climate.copernicus.eu/cdsapp#!/dataset/cems-fire-historical?tab=overview>).

865 **Supplementary information**

866 The supplement related to this article is available online at doi:

867 **Author contribution**

868 T.D. Hessilt designed the study with input from B.M. Rogers, R.C. Scholten and S. Veraverbeke. T.D.
869 Hessilt performed the analyses and wrote the manuscript with inputs from all authors.

870 **Competing interests**

871 The authors declare no competing interests.

872 **Acknowledgements**

873 This work was carried out under the umbrella of the Netherlands Earth System Science Centre (NESSC).
874 This project has received funding from the European Union's Horizon 2020 research and innovation
875 programme under the Marie Skłodowska-Curie, Grant Agreement No. 847504. The contribution of
876 R.C.S. was partly funded by the Dutch Research Council through Vidi grant 016.Vidi.189.070 awarded to
877 S.V. The contributions of R.C.S and T.A.J. ~~were~~ funded by the European Research Council through a
878 Consolidator grant under the European Union's Horizon 2020 research and innovation program (grant
879 agreement No. 101000987) awarded to S.V. B.M.R. acknowledges funding from the NASA Arctic-
880 Boreal Vulnerability Experiment (NNX15AU56A), the Gordon and Betty Moore Foundation (grant
881 #8414), and funding catalyzed through the Audacious Project. ~~The authors.~~ ~~D.H~~ would like to thank D.

882 Coumou for fruitful discussions on the effect of land-atmosphere dynamics related to ~~snowmelt~~snow
883 disappearance.

884 **References**

- 885 Abatzoglou, J. T. and Williams, A. P.: Impact of anthropogenic climate change on wildfire across western US forests, *Proc. Natl.*
886 *Acad. Sci. U. S. A.*, 113, 11770–11775, <https://doi.org/10.1073/pnas.1607171113>, 2016.
- 887 Abatzoglou, J. T., Kolden, C. A., Balch, J. K., and Bradley, B. A.: Controls on interannual variability in lightning-caused fire
888 activity in the western US, *Environ. Res. Lett.*, 11, <https://doi.org/10.1088/1748-9326/11/4/045005>, 2016.
- 889 Albert-Green, A., Dean, C. B., Martell, D. L., and Woolford, D. G.: A methodology for investigating trends in changes in the
890 timing of the fire season with applications to lightning-caused forest fires in Alberta and Ontario, Canada, *Can. J. For. Res.*, 43,
891 39–45, <https://doi.org/10.1139/cjfr-2011-0432>, 2013.
- 892 Alves, M., Nadeau, D. F., Music, B., Ancil, F., and Parajuli, A.: On the performance of the Canadian land surface scheme driven
893 by the ERA5 reanalysis over the Canadian boreal forest, *J. Hydrometeorol.*, 21, 1383–1404, [https://doi.org/10.1175/JHM-D-19-](https://doi.org/10.1175/JHM-D-19-0172.1)
894 [0172.1](https://doi.org/10.1175/JHM-D-19-0172.1), 2020.
- 895 Anisimov, O. A., Vaughan, D. G., Callaghan, T. V., Furgal, C., Marchant, H., Prowse, T. D., Vilhjalmsson, H., and Walsh, J. E.:
896 Polar regions (Arctic and Antarctic), *Clim. Chang. 2007 Impacts, Adapt. Vulnerability. Contrib. of Working Gr. II to Fourth As-*
897 *essment Rep. Intergov. Panel Clim. Chang.*, 653–685, 2007.
- 898 Armstrong, A., Braaten, J., and Shelby, M.: Identifying Annual First Day of No Snow Cover, Google Earth Engine, 2023.
- 899 Balshi, M. S., McGuire, A. D., Duffy, P., Flannigan, M., Walsh, J., and Melillo, J.: Assessing the response of area burned to
900 changing climate in western boreal North America using a Multivariate Adaptive Regression Splines (MARS) approach, *Glob.*
901 *Chang. Biol.*, 15, 578–600, <https://doi.org/10.1111/j.1365-2486.2008.01679.x>, 2009.
- 902 Baltzer, J. L., Day, N. J., Walker, X. J., Greene, D., Mack, M. C., Alexander, H. D., Arseneault, D., Barnes, J., Bergeron, Y.,
903 Boucher, Y., Bourgeau-Chavez, L., Brown, C. D., Carriere, S., Howard, B. K., Gauthier, S., Parisien, M. A., Reid, K. A., Rogers,
904 B. M., Roland, C., Sirois, L., Stehn, S., Thompson, D. K., Turetsky, M. R., Veraverbeke, S., Whitman, E., Yang, J., and
905 Johnstone, J. F.: Increasing fire and the decline of fire adapted black spruce in the boreal forest, *Proc. Natl. Acad. Sci. U. S. A.*,
906 118, 1–9, <https://doi.org/10.1073/pnas.2024872118>, 2021.
- 907 Barnett, T. P., Adam, J. C., and Lettenmaier, D. P.: Potential impacts of a warming climate on water availability in snow-
908 dominated regions, *Nature*, 438, 303–309, <https://doi.org/10.1038/nature04141>, 2005.
- 909 Bartsch, A., Baltzer, H., and George, C.: The influence of regional surface soil moisture anomalies on forest fires in Siberia
910 observed from satellites, *Environ. Res. Lett.*, 4, <https://doi.org/10.1088/1748-9326/4/4/045021>, 2009.

911 Bormann, K. J., Brown, R. D., Derksen, C., and Painter, T. H.: Estimating snow-cover trends from space, *Nat. Clim. Chang.*, 8,
912 924–928, <https://doi.org/10.1038/s41558-018-0318-3>, 2018.

913 Brodzik, M. J. and Armstrong, R.: Northern Hemisphere EASE-Grid 2.0 Weekly Snow Cover and Sea Ice Extent, Version 4,
914 NASA Natl. Snow Ice Data Cent. Distrib. Act. Arch. Cent., 2013.

915 Brown, R. D. and Mote, P. W.: The response of Northern Hemisphere snow cover to a changing climate, *J. Clim.*, 22, 2124–
916 2145, <https://doi.org/10.1175/2008JCLI2665.1>, 2009.

917 Brown, R. D. and Robinson, D. A.: Northern Hemisphere spring snow cover variability and change over 1922–2010 including an
918 assessment of uncertainty, *Cryosphere*, 5, 219–229, <https://doi.org/10.5194/tc-5-219-2011>, 2011.

919 Buermann, W., Bikash, P. R., Jung, M., Burn, D. H., and Reichstein, M.: Earlier springs decrease peak summer productivity in
920 North American boreal forests, *Environ. Res. Lett.*, 8, <https://doi.org/10.1088/1748-9326/8/2/024027>, 2013.

921 Chen, X., Liang, S., and Cao, Y.: Satellite observed changes in the Northern Hemisphere snow cover phenology and the
922 associated radiative forcing and feedback between 1982 and 2013, *Environ. Res. Lett.*, 11, <https://doi.org/10.1088/1748-9326/11/8/084002>, 2016.

924 Chen, Y., Romps, D. M., Seeley, J. T., Veraverbeke, S., Riley, W. J., Mekonnen, Z. A., and Randerson, J. T.: Future increases in
925 Arctic lightning and fire risk for permafrost carbon, *Nat. Clim. Chang.*, 11, 404–410, [https://doi.org/10.1038/s41558-021-01011-](https://doi.org/10.1038/s41558-021-01011-y)
926 y, 2021.

927 Cohen, J., Screen, J. A., Furtado, J. C., Barlow, M., Whittleston, D., Coumou, D., Francis, J., Dethloff, K., Entekhabi, D.,
928 Overland, J., and Jones, J.: Recent Arctic amplification and extreme mid-latitude weather, *Nat. Geosci.*, 7, 627–637,
929 <https://doi.org/10.1038/ngeo2234>, 2014.

930 Cohen, J. L., Furtado, J. C., Barlow, M. A., Alexeev, V. A., and Cherry, J. E.: Arctic warming, increasing snow cover and
931 widespread boreal winter cooling, *Environ. Res. Lett.*, 7, <https://doi.org/10.1088/1748-9326/7/1/014007>, 2012.

932 Coumou, D., Di Capua, G., Vavrus, S., Wang, L., and Wang, S.: The influence of Arctic amplification on mid-latitude summer
933 circulation, *Nat. Commun.*, 9, 1–12, <https://doi.org/10.1038/s41467-018-05256-8>, 2018.

934 Déry, S. J. and Brown, R. D.: Recent Northern Hemisphere snow cover extent trends and implications for the snow-albedo
935 feedback, *Geophys. Res. Lett.*, 34, 1–6, <https://doi.org/10.1029/2007GL031474>, 2007.

936 Estilow, T. W., Young, A. H., and Robinson, D. A.: A long-term Northern Hemisphere snow cover extent data record for climate
937 studies and monitoring, *Earth Syst. Sci. Data*, 7, 137–142, <https://doi.org/10.5194/essd-7-137-2015>, 2015.

938 Flanner, M. G., Shell, K. M., Barlage, M., Perovich, D. K., and Tschudi, M. A.: Radiative forcing and albedo feedback from the
939 Northern Hemisphere cryosphere between 1979 and 2008, *Nat. Geosci.*, 4, 151–155, <https://doi.org/10.1038/ngeo1062>, 2011.

940 Flannigan, M., Cantin, A. S., De Groot, W. J., Wotton, M., Newbery, A., and Gowman, L. M.: Global wildland fire season
941 severity in the 21st century, *For. Ecol. Manage.*, 294, 54–61, <https://doi.org/10.1016/j.foreco.2012.10.022>, 2013.

942 Flannigan, M. D., Logan, K. A., Amiro, B. D., Skinner, W. R., and Stocks, B. J.: Future area burned in Canada, *Clim. Change*,
943 72, 1–16, <https://doi.org/10.1007/s10584-005-5935-y>, 2005.

944 Flannigan, M. D., Wotton, B. M., Marshall, G. A., de Groot, W. J., Johnston, J., Jurko, N., and Cantin, A. S.: Fuel moisture
945 sensitivity to temperature and precipitation: climate change implications, *Clim. Change*, 134, 59–71,
946 <https://doi.org/10.1007/s10584-015-1521-0>, 2016.

947 Francis, J. A. and Vavrus, S. J.: Evidence linking Arctic amplification to extreme weather in mid-latitudes, *Geophys. Res. Lett.*,
948 39, 1–6, <https://doi.org/10.1029/2012GL051000>, 2012.

949 French, N. H. F., Jenkins, L. K., Loboda, T. V., Flannigan, M., Jandt, R., Bourgeau-Chavez, L. L., and Whitley, M.: Fire in arctic
950 tundra of Alaska: Past fire activity, future fire potential, and significance for land management and ecology, *Int. J. Wildl. Fire*,
951 24, 1045–1061, <https://doi.org/10.1071/WF14167>, 2015.

952 Gergel, D. R., Nijssen, B., Abatzoglou, J. T., Lettenmaier, D. P., and Stumbaugh, M. R.: Effects of climate change on snowpack
953 and fire potential in the western USA, *Clim. Change*, 141, 287–299, <https://doi.org/10.1007/s10584-017-1899-y>, 2017.

954 Giglio, L., Schroeder, W., and Justice, C. O.: The collection 6 MODIS active fire detection algorithm and fire products, *Remote*
955 *Sens. Environ.*, 178, 31–41, <https://doi.org/10.1016/j.rse.2016.02.054>, 2016.

956 Giglio, L., Boschetti, L., Roy, D. P., Humber, M. L., and Justice, C. O.: The Collection 6 MODIS burned area mapping algorithm
957 and product, *Remote Sens. Environ.*, 217, 72–85, <https://doi.org/10.1016/j.rse.2018.08.005>, 2018.

958 Gloege, L., Kornhuber, K., Skulovich, O., Pal, I., Zhou, S., Ciais, P., and Gentine, P.: Land-Atmosphere Cascade Fueled the 2020
959 Siberian Heatwave, *AGU Adv.*, 3, <https://doi.org/10.1029/2021AV000619>, 2022.

960 Goss, M., Swain, D. L., Abatzoglou, J. T., Sarhadi, A., Kolden, C. A., Williams, A. P., and Diffenbaugh, N. S.: Climate change is
961 increasing the likelihood of extreme autumn wildfire conditions across California, *Environ. Res. Lett.*, 15,
962 <https://doi.org/10.1088/1748-9326/ab83a7>, 2020.

963 Graham, R. M., Cohen, L., Petty, A. A., Boisvert, L. N., Rinke, A., Hudson, S. R., Nicolaus, M., and Granskog, M. A.: Increasing
964 frequency and duration of Arctic winter warming events, *Geophys. Res. Lett.*, 44, 6974–6983,

965 <https://doi.org/10.1002/2017GL073395>, 2017.

966 Groisman, P. Y., Karl, T. R., and Knight, R. W.: Observed impact of snow cover on the heat balance and the rise of continental
967 spring temperatures, *Science* (80-.), 263, 198–200, <https://doi.org/10.1126/science.263.5144.198>, 1994.

968 Hall, D. K. and Riggs, G. A.: MODIS/Terra Snow Cover Daily L3 Global 500m Grid, Version 6, Boulder, Color. USA Natl.
969 Snow Ice Data Cent., <https://doi.org/https://doi.org/10.5067/MODIS/MOD10A1.006>, 2016.

970 Hanes, C. C., Wang, X., Jain, P., Parisien, M. A., Little, J. M., and Flannigan, M. D.: Fire-regime changes in canada over the last
971 half century, *Can. J. For. Res.*, 49, 256–269, <https://doi.org/10.1139/cjfr-2018-0293>, 2019.

972 Helfrich, S. R., McNamara, D., Ramsay, B. H., Baldwin, T., and Kasheta, T.: Enhancements to, and forthcoming developments
973 in the Interactive Multisensor Snow and Ice Mapping System (IMS), *Hydrol. Process.*, 21, 1576–1586,
974 <https://doi.org/10.1002/hyp.6720>, 2007.

975 Hersbach, H., Bell, B., Berrisford, P., Hirahara, S., Horányi, A., Muñoz-Sabater, J., Nicolas, J., Peubey, C., Radu, R., Schepers,
976 D., Simmons, A., Soci, C., Abdalla, S., Abellan, X., Balsamo, G., Bechtold, P., Biavati, G., Bidlot, J., Bonavita, M., De Chiara,
977 G., Dahlgren, P., Dee, D., Diamantakis, M., Dragani, R., Flemming, J., Forbes, R., Fuentes, M., Geer, A., Haimberger, L., Healy,
978 S., Hogan, R. J., Hólm, E., Janisková, M., Keeley, S., Laloyaux, P., Lopez, P., Lupu, C., Radnoti, G., de Rosnay, P., Rozum, I.,
979 Vamborg, F., Villaume, S., and Thépaut, J. N.: The ERA5 global reanalysis, *Q. J. R. Meteorol. Soc.*, 146, 1999–2049,
980 <https://doi.org/10.1002/qj.3803>, 2020.

981 Hessilt, T. D., Abatzoglou, J. T., Chen, Y., Randerson, J. T., Scholten, R. C., Van Der Werf, G., and Veraverbeke, S.: Future
982 increases in lightning ignition efficiency and wildfire occurrence expected from drier fuels in boreal forest ecosystems of western
983 North America, *Environ. Res. Lett.*, 17, <https://doi.org/10.1088/1748-9326/ac6311>, 2022.

984 Holden, Z. A., Swanson, A., Luce, C. H., Jolly, W. M., Maneta, M., Oyler, J. W., Warren, D. A., Parsons, R., and Affleck, D.:
985 Decreasing fire season precipitation increased recent western US forest wildfire activity, *Proc. Natl. Acad. Sci. U. S. A.*, 115,
986 E8349–E8357, <https://doi.org/10.1073/pnas.1802316115>, 2018.

987 Horton, R. M., Mankin, J. S., Lesk, C., Coffel, E., and Raymond, C.: A Review of Recent Advances in Research on Extreme
988 Heat Events, *Curr. Clim. Chang. Reports*, 2, 242–259, <https://doi.org/10.1007/s40641-016-0042-x>, 2016.

989 Jain, P. and Flannigan, M.: The relationship between the polar jet stream and extreme wildfire events in North America, *J. Clim.*,
990 34, 6247–6265, <https://doi.org/10.1175/JCLI-D-20-0863.1>, 2021.

991 Jain, P., Wang, X., and Flannigan, M. D.: Trend analysis of fire season length and extreme fire weather in North America

992 between 1979 and 2015, *Int. J. Wildl. Fire*, 26, 1009–1020, <https://doi.org/10.1071/WF17008>, 2017.

993 Jolly, W. M., Cochrane, M. A., Freeborn, P. H., Holden, Z. A., Brown, T. J., Williamson, G. J., and Bowman, D. M. J. S.:
994 Climate-induced variations in global wildfire danger from 1979 to 2013, *Nat. Commun.*, 6, 1–11,
995 <https://doi.org/10.1038/ncomms8537>, 2015.

996 Justice, C. O., Giglio, L., Korontzi, S., Owens, J., Morisette, J. T., Roy, D., Descloitres, J., Alleaume, S., Petitcolin, F., and
997 Kaufman, Y.: The MODIS fire products, *Remote Sens. Environ.*, 83, 244–262, [https://doi.org/10.1016/S0034-4257\(02\)00076-7](https://doi.org/10.1016/S0034-4257(02)00076-7),
998 2002.

999 Kasischke, E. S., Williams, D., and Barry, D.: Analysis of the patterns of large fires in the boreal forest region of Alaska, *Int. J.*
1000 *Wildl. Fire*, 11, 131–144, <https://doi.org/10.1071/WF02023>, 2002.

1001 Kim, B. M., Son, S. W., Min, S. K., Jeong, J. H., Kim, S. J., Zhang, X., Shim, T., and Yoon, J. H.: Weakening of the
1002 stratospheric polar vortex by Arctic sea-ice loss, *Nat. Commun.*, 5, <https://doi.org/10.1038/ncomms5646>, 2014.

1003 Kitzberger, T., Falk, D. A., Westerling, A. L., and Swetnam, T. W.: Direct and indirect climate controls predict heterogeneous
1004 early-mid 21st century wildfire burned area across western and boreal North America, *PLoS One*, 12, 429–438,
1005 <https://doi.org/10.1371/journal.pone.0188486>, 2017.

1006 Kretschmer, M., Coumou, D., Agel, L., Barlow, M., Tziperman, E., and Cohen, J. D.: More-persistent weak stratospheric polar
1007 vortex States linked to cold extremes, *Bull. Am. Meteorol. Soc.*, 99, 49–60, <https://doi.org/10.1175/BAMS-D-16-0259.1>, 2018a.

1008 Kretschmer, M., Cohen, J., Matthias, V., Runge, J., and Coumou, D.: The different stratospheric influence on cold-extremes in
1009 Eurasia and North America, *npj Clim. Atmos. Sci.*, 1, 1–10, <https://doi.org/10.1038/s41612-018-0054-4>, 2018b.

1010 Lawson, B. D. and Armitage, O. B.: *Weather Guide Canadian Forest Fire Danger Rating System*, 1–73 pp., 2008.

1011 Lefcheck, J. S.: piecewiseSEM: Piecewise structural equation modelling in r for ecology, evolution, and systematics, *Methods*
1012 *Ecol. Evol.*, 7, 573–579, <https://doi.org/10.1111/2041-210X.12512>, 2016.

1013 Li, D., Wrzesien, M. L., Durand, M., Adam, J., and Lettenmaier, D. P.: How much runoff originates as snow in the western
1014 United States, and how will that change in the future?, *Geophys. Res. Lett.*, 44, 6163–6172,
1015 <https://doi.org/10.1002/2017GL073551>, 2017.

1016 Liu, L., Gudmundsson, L., Hauser, M., Qin, D., Li, S., and Seneviratne, S. I.: Soil moisture dominates dryness stress on
1017 ecosystem production globally, *Nat. Commun.*, 11, 1–9, <https://doi.org/10.1038/s41467-020-18631-1>, 2020.

1018 Mann, H. B. and Whitney, D. R.: On a Test of Whether one of Two Random Variables is Stochastically Larger than the Other,

- 1019 Ann. Math. Stat., 1, 50–60, 1947.
- 1020 McCabe, G. J., Clark, M. P., and Hay, L. E.: Rain-on-snow events in the western United States, Bull. Am. Meteorol. Soc., 88,
1021 319–328, <https://doi.org/10.1175/BAMS-88-3-319>, 2007.
- 1022 McCammon, B. P.: Snowpack influences on dead fuel moisture, For. Sci., 22, 323–328, 1976.
- 1023 McCarty, J. L., Smith, T. E. L., and Turetsky, M. R.: Arctic fires re-emerging, Nat. Geosci., 13, 658–660,
1024 <https://doi.org/10.1038/s41561-020-00645-5>, 2020.
- 1025 McCoy, C. and Neumark-Gaudet, L.: 9. Commission for Environmental Cooperation (CEC), Yearb. Int. Environ. Law,
1026 <https://doi.org/10.1093/yiel/yvac036>, 2022.
- 1027 Miles, V. V. and Esau, I.: Spatial heterogeneity of greening and browning between and within bioclimatic zones in northern West
1028 Siberia, Environ. Res. Lett., 11, <https://doi.org/10.1088/1748-9326/11/11/115002>, 2016.
- 1029 Oksanen, J., Blanchet, F. G., Kindt, R., Legendre, P., Minchin, P. R., O'hara, R. B., ..., and Oksanen, M. J.: Package 'vegan'.
1030 Community ecology package, version, 2(9), 1-295., 2013.
- 1031 Olthof, I., Latifovic, R., and Pouliot, D.: Medium resolution land cover mapping of Canada from SPOT 4/5 data, Tech. Report,
1032 Geomatics Canada, 2015, <https://doi.org/10.4095/295751>, 2015.
- 1033 Omernik, J. M.: Ecoregions of the Conterminous United States, Ann. Assoc. Am. Geogr., 77, 118–125,
1034 <https://doi.org/10.1111/j.1467-8306.1987.tb00149.x>, 1987.
- 1035 Omernik, J. M.: Ecoregions: a framework for managing ecosystems, 1995.
- 1036 Parisien, M. A., Barber, Q. E., Flannigan, M. D., and Jain, P.: Broadleaf tree phenology and springtime wildfire occurrence in
1037 boreal Canada, Glob. Chang. Biol., 1–14, <https://doi.org/10.1111/gcb.16820>, 2023.
- 1038 Pavlic, G., Chen, W., Fernandes, R., Cihlar, J., Price, D. T., Latifovic, R., Fraser, R., Chen, W., Fernandes, R., Cihlar, J., Price,
1039 D. T., Latifovic, R., and Fraser, R.: Canada-wide maps of dominant tree species from remotely sensed and ground data, Geocarto
1040 Int., 22, 185–207, <https://doi.org/10.1080/10106040701201798>, 2007.
- 1041 Phillips, C. A., Rogers, B. M., Elder, M., Cooperdock, S., Moubarak, M., Randerson, J. T., and Frumhoff, P. C.: Escalating
1042 carbon emissions from North American boreal forest wildfires and the climate mitigation potential of fire management, Sci.
1043 Adv., 8, <https://doi.org/10.1126/sciadv.abl7161>, 2022.
- 1044 Pinheiro, J., Bates, D., and Team, R. C.: nlme: Linear and Nonlinear Mixed Effects Models version 3.1-160, <https://cran.r->

1045 project.org/package=nlme, 2022.

1046 Post, E., Forchhammer, M. C., Bret-Harte, M. S., Callaghan, T. V., Christensen, T. R., Elberling, B., Fox, A. D., Gilg, O., Hik, D.
1047 S., Høye, T. T., Ims, R. A., Jeppesen, E., Klein, D. R., Madsen, J., McGuire, A. D., Rysgaard, S., Schindler, D. E., Stirling, I.,
1048 Tamstorf, M. P., Tyler, N. J. C., Van Der Wal, R., Welker, J., Wookey, P. A., Schmidt, N. M., and Aastrup, P.: Ecological
1049 dynamics across the arctic associated with recent climate change, *Science* (80-.), 325, 1355–1358,
1050 <https://doi.org/10.1126/science.1173113>, 2009.

1051 Potter, S., Cooperdock, S., Veraverbeke, S., Walker, X., Mack, M. C., Goetz, S. J., Baltzer, J., Bourgeau-Chavez, L., Burrell, A.,
1052 Dieleman, C., French, N., Hantson, S., Hoy, E. E., Jenkins, L., Johnstone, J. F., Natali, S. M., Randerson, J. T., Turetsky, M. R.,
1053 Whitman, E., Wiggins, E., and Rogers, B. M.: Burned Area and Carbon Emissions Across Northwestern Boreal North America
1054 from 2001-2019, *Biogeosciences*, 20, <https://doi.org/10.5194/bg-20-2785-2023>, 2023.

1055 Ramsay, B. H.: The interactive multisensor snow and ice mapping system, *Hydrol. Process.*, 12, 1537–1546,
1056 [https://doi.org/10.1002/\(sici\)1099-1085\(199808/09\)12:10/11<1537::aid-hyp679>3.0.co;2-a](https://doi.org/10.1002/(sici)1099-1085(199808/09)12:10/11<1537::aid-hyp679>3.0.co;2-a), 1998.

1057 Rantanen, M., Karpechko, A. Y., Lipponen, A., Nordling, K., Hyvärinen, O., Ruosteenoja, K., Vihma, T., and Laaksonen, A.:
1058 The Arctic has warmed nearly four times faster than the globe since 1979, *Commun. Earth Environ.*, 3, 1–10,
1059 <https://doi.org/10.1038/s43247-022-00498-3>, 2022.

1060 Robinson, D., David, A., Estilow, T., and Program, N. C.: NOAA Climate Data Record (CDR) of Northern Hemisphere (NH)
1061 Snow Cover Extent (SCE), Version 1., NOAA Natl. Clim. Data Cent., 137–142, <https://doi.org/10.7289/V5N014G9>, 2012.

1062 Salomonson, V. V. and Appel, I.: Estimating fractional snow cover from MODIS using the normalized difference snow index,
1063 *Remote Sens. Environ.*, 89, 351–360, <https://doi.org/10.1016/j.rse.2003.10.016>, 2004.

1064 Scholten, R. C., Veraverbeke, S., Jandt, R., Miller, E. A., and Rogers, B. M.: ABoVE: Ignitions, Burned Area, and Emissions of
1065 Fires in AK, YT, and NWT, 2001-2018, ORNL DAAC, Oak Ridge, Tennessee, USA,
1066 <https://doi.org/https://doi.org/10.3334/ORNLDAAC/1812>, 2021a.

1067 Scholten, R. C., Jandt, R., Miller, E. A., Rogers, B. M., and Veraverbeke, S.: Overwintering fires in boreal forests, *Nature*, 593,
1068 399–404, <https://doi.org/10.1038/s41586-021-03437-y>, 2021b.

1069 Scholten, R. C., Coumou, D., Luo, F., and Veraverbeke, S.: Early snowmelt and polar jet dynamics co-influence recent extreme
1070 Siberian fire seasons, *Science* (80-.), 1009, 1005–1009, <https://doi.org/10.1126/science.abn4419>, 2022.

1071 Sedano, F. and Randerson, J. T.: Multi-scale influence of vapor pressure deficit on fire ignition and spread in boreal forest

1072 ecosystems, *Biogeosciences*, 11, 3739–3755, <https://doi.org/10.5194/bg-11-3739-2014>, 2014.

1073 Seneviratne, S. I., Corti, T., Davin, E. L., Hirschi, M., Jaeger, E. B., Lehner, I., Orlowsky, B., and Teuling, A. J.: Investigating
1074 soil moisture-climate interactions in a changing climate: A review, *Earth-Science Rev.*, 99, 125–161,
1075 <https://doi.org/10.1016/j.earscirev.2010.02.004>, 2010.

1076 Sharma, A. R., Jain, P., Abatzoglou, J. T., and Flannigan, M.: Persistent Positive Anomalies in Geopotential Heights Promote
1077 Wildfires in Western North America, *J. Clim.*, 35, 2867–2884, <https://doi.org/10.1175/JCLI-D-21-0926.1>, 2022.

1078 Shipley, B.: Confirmatory path analysis in a generalized multilevel context, *Ecology*, 90, 363–368, <https://doi.org/10.1890/08-1034.1>, 2009.

1080 Singh, D., Swain, D. L., Mankin, J. S., Horton, D. E., Thomas, L. N., Rajaratnam, B., and Diffenbaugh, N. S.: Recent
1081 amplification of the North American winter temperature dipole, *J. Geophys. Res.*, 121, 9911–9928,
1082 <https://doi.org/10.1002/2016JD025116>, 2016.

1083 Skakun, R., Whitman, E., Little, J. M., and Parisien, M. A.: Area burned adjustments to historical wildland fires in Canada,
1084 *Environ. Res. Lett.*, 16, <https://doi.org/10.1088/1748-9326/abfb2c>, 2021.

1085 Skinner, W. R., Stocks, B. J., Martell, D. L., Bonsal, B., and Shabbar, A.: The association between circulation anomalies in the
1086 mid-troposphere and area burned by wildland fire in Canada, *Theor. Appl. Climatol.*, 63, 89–105,
1087 <https://doi.org/10.1007/s007040050095>, 1999.

1088 Stocks, B. J., Mason, J. A., Todd, J. B., Bosch, E. M., Wotton, B. M., Amiro, B. D., Flannigan, M. D., Hirsch, K. G., Logan, K.
1089 A., Martell, D. L., and Skinner, W. R.: Large forest fires in Canada, 1959–1997, *J. Geophys. Res. Atmos.*, 108,
1090 <https://doi.org/10.1029/2001jd000484>, 2002.

1091 Suzuki, K., Hiyama, T., Matsuo, K., Ichii, K., Iijima, Y., and Yamazaki, D.: Accelerated continental-scale snowmelt and
1092 ecohydrological impacts in the four largest Siberian river basins in response to spring warming, *Hydrol. Process.*, 34, 3867–3881,
1093 <https://doi.org/10.1002/hyp.13844>, 2020.

1094 Swenson, S. C. and Lawrence, D. M.: A new fractional snow-covered area parameterization for the Community Land Model and
1095 its effect on the surface energy balance, *J. Geophys. Res. Atmos.*, 117, 1–20, <https://doi.org/10.1029/2012JD018178>, 2012.

1096 Tang, Q., Zhang, X., and Francis, J. A.: Extreme summer weather in northern mid-latitudes linked to a vanishing cryosphere, *Nat.*
1097 *Clim. Chang.*, 4, 45–50, <https://doi.org/10.1038/nclimate2065>, 2014.

1098 Team, R. D. C.: R: a language and environment for statistical computing, 2022.

- 1099 USEPA: Ecoregions of North America, 2015.
- 1100 Veraverbeke, S., Rogers, B. M., and Randerson, J. T.: Daily burned area and carbon emissions from boreal fires in Alaska,
1101 Biogeosciences, 12, 3579–3601, <https://doi.org/10.5194/bg-12-3579-2015>, 2015.
- 1102 Veraverbeke, S., Rogers, B. M., Goulden, M. L., Jandt, R. R., Miller, C. E., Wiggins, E. B., and Randerson, J. T.: Lightning as a
1103 major driver of recent large fire years in North American boreal forests, *Nat. Clim. Chang.*, 7, 529–534,
1104 <https://doi.org/10.1038/nclimate3329>, 2017.
- 1105 Verbyla, D. L.: ABoVE: Last Day of Spring Snow, Alaska, USA, and Yukon Territory, Canada, 2000-2016, ORNL DAAC, 1,
1106 <https://doi.org/doi.org/10.3334/ORNLDAAC/1528>, 2017.
- 1107 Vitolo, C., Di Giuseppe, F., Barnard, C., Coughlan, R., San-Miguel-Ayanz, J., Libertá, G., and Krzeminski, B.: ERA5-based
1108 global meteorological wildfire danger maps, *Sci. Data*, 7, 1–11, <https://doi.org/10.1038/s41597-020-0554-z>, 2020.
- 1109 Van Wagner, C. E.: Development and Structure of the Canadian Forest Fire Weather Index System, 37 pp., 1987.
- 1110 Westerling, A. L., Hidalgo, H. G., Cayan, D. R., and Swetnam, T. W.: Warming and earlier spring increase Western U.S. forest
1111 wildfire activity, *Science (80-.)*, 313, 940–943, <https://doi.org/10.1126/science.1128834>, 2006.
- 1112 Wotton, B. M. and Flannigan, M. D.: Length of the fire season in a changing climate, *For. Chron.*, 69, 187–192,
1113 <https://doi.org/10.5558/tfc69187-2>, 1993.
- 1114 Wotton, B. M., Nock, C. A., and Flannigan, M. D.: Forest fire occurrence and climate change in Canada, *Int. J. Wildl. Fire*, 19,
1115 253–271, <https://doi.org/10.1071/WF09002>, 2010.
- 1116 Xu, W., Scholten, R. C., Hessilt, T. D., Liu, Y., and Veraverbeke, S.: Overwintering fires rising in eastern Siberia, *Environ. Res.*
1117 *Lett.*, 17, <https://doi.org/10.1088/1748-9326/ac59aa>, 2022.
- 1118 Zhao, Z., Lin, Z., Li, F., and Rogers, B. M.: Influence of atmospheric teleconnections on interannual variability of Arctic-boreal
1119 fires, *Sci. Total Environ.*, 838, 156550, <https://doi.org/10.1016/j.scitotenv.2022.156550>, 2022.
- 1120 Zona, D., Lafleur, P. M., Hufkens, K., Bailey, B., Gioli, B., Burba, G., Goodrich, J. P., Liljedahl, A. K., Euskirchen, E. S., Watts,
1121 J. D., Farina, M., Kimball, J. S., Heimann, M., Göckede, M., Pallandt, M., Christensen, T. R., Mastepanov, M., López-Blanco, E.,
1122 Jackowicz-Korczynski, M., Dolman, A. J., Marchesini, L. B., Commane, R., Wofsy, S. C., Miller, C. E., Lipson, D. A., Hashemi,
1123 J., Arndt, K. A., Kutzbach, L., Holl, D., Boike, J., Wille, C., Sachs, T., Kalhori, A., Song, X., Xu, X., Humphreys, E. R., Koven,
1124 C. D., Sonntag, O., Meyer, G., Gosselin, G. H., Marsh, P., and Oechel, W. C.: Earlier snowmelt may lead to late season
1125 declines in plant productivity and carbon sequestration in Arctic tundra ecosystems, *Sci. Rep.*, 12, 1–10,

- 1126 <https://doi.org/10.1038/s41598-022-07561-1>, 2022.
- 1127 Zou, Y., Rasch, P. J., Wang, H., Xie, Z., and Zhang, R.: Increasing large wildfires over the western United States linked to
- 1128 diminishing sea ice in the Arctic, *Nat. Commun.*, 12, 1–12, <https://doi.org/10.1038/s41467-021-26232-9>, 2021.
- 1129 Zuur, A. F., Ieno, E. N., Walker, N. J., Saveliev, A. A., and Smith, G. M.: *Mixed effects models and extensions in ecology with*
- 1130 *R*, Springer New York, NY, 574 pp., <https://doi.org/https://doi.org/10.1007/978-0-387-87458-6>, 2009.
- 1131